

On the Intermittent Formation of an Ice Bridge (*Nunniq*) across Roes Welcome Sound, Northwestern Hudson Bay and Its Use to Local Inuit Hunters

David G. Babb,^{1,2} Sergei Kirillov,¹ Zou Zou A. Kuzyk,¹ Troy Netser,³ Jasmine Liesch,^{1,4} C. Michelle Kamula,¹ Tom Zagon,⁵ David G. Barber¹ and Jens K. Ehn¹

(Received 28 May 2021; accepted in revised form 8 October 2021)

ABSTRACT. Ice bridges are unique features that form when sea ice consolidates and remains immobilized within channels. They form in many locations throughout the Arctic and are typically noted for the polynyas that form on their lee side. However, ice bridges also provide a temporary platform that may be used by both humans and wildlife to cross otherwise impassable channels. For generations, Inuit in Coral Harbour, Nunavut, have used an ice bridge to cross Roes Welcome Sound and expand their hunting territory, though they report that the bridge only forms approximately every four years. Of interest both to Inuit and the scientific community is why the bridge forms so intermittently, by what mechanisms, and whether the frequency will change with ongoing warming and sea ice loss. Using satellite imagery, we determined that the bridge formed during 14 of the past 50 years (1971–2020). Generally, the bridge forms between January and March during a cold period that coincides with neap tide and after surface winds have rotated from the prevailing northerly (along-channel) winds to west-northwesterly (across-channel) winds. This rotation compresses the existing ice pack against Southampton Island, where it remains stationary because of the calm along-channel winds and low tidal range and coalesces under cold air temperatures. Breakup occurs between mid-June and early July after the onset of melt. Overall, the bridge forms when a specific set of conditions occur simultaneously; however, a warming climate, specifically a reduction in very cold days and a shorter ice season may affect the frequency of bridge formation, thereby limiting Inuit travel.

Key words: sea ice; ice bridge; Roes Welcome Sound; Nunavut; Kivalliq; Hudson Bay; Inuit knowledge; remote sensing

RÉSUMÉ. Les ponts de glace sont des caractéristiques uniques qui se forment lorsque la glace de mer se consolide et reste immobilisée dans les chenaux. Ils se forment en maint endroit de l'Arctique et se démarquent généralement par les polynyas qui se créent de leur côté sous le vent. Cependant, les ponts de glace font aussi office de plateforme temporaire dont peuvent se servir tant les humains que la faune pour traverser des chenaux qui seraient autrement impraticables. Depuis des générations, les Inuits de Coral Harbour, au Nunavut, empruntent un pont de glace pour traverser le détroit de Roes Welcome et agrandir leur territoire de chasse, même si selon eux, ce pont ne se forme qu'aux quatre ans environ. Les Inuits et les scientifiques se demandent pourquoi le pont se forme de manière si intermittente, grâce à quels mécanismes ils apparaissent, et si la fréquence de formation des ponts va changer en raison du réchauffement continu et de la perte de glace de mer. À l'aide d'imagerie satellitaire, nous avons déterminé qu'un pont s'est formé durant 14 des 50 dernières années (1971–2020). De manière générale, le pont apparaît entre janvier et mars pendant une période froide qui coïncide avec la marée de morte-eau, après la rotation des vents de surface, qui passent des vents dominants du nord (longeant le chenal) aux vents de l'ouest-nord-ouest (traversant le chenal). Cette rotation a pour effet de comprimer la banquise actuelle contre l'île Southampton, où elle demeure stationnaire en raison des vents calmes longeant le chenal et de la faible amplitude de la marée, et où elle coalesce sous les froides températures de l'air. La dislocation se produit entre la mi-juin et le début de juillet, après le début de la fonte des glaces. Dans l'ensemble, le pont se forme lorsque certaines conditions se manifestent simultanément. Toutefois, le réchauffement climatique, plus précisément en ce qui a trait à la réduction du nombre de journées très froides et au raccourcissement de la saison des glaces, pourrait avoir un effet sur la fréquence de la formation du pont, ce qui limiterait les déplacements des Inuits.

Mots clés : glace de mer; pont de glace; détroit de Roes Welcome; Nunavut; Kivalliq; baie d'Hudson; connaissances des Inuits; télédétection

Traduit pour la revue *Arctic* par Nicole Giguère.

¹ Centre for Earth Observation Science, 125 Dysart Road, University of Manitoba, Winnipeg, Manitoba R3T 2N2, Canada

² Corresponding author: david.babb@umanitoba.ca

³ Coral Harbour, Nunavut X0C 0C0, Canada

⁴ Department of Anthropology, 15 Chancellors Circle, University of Manitoba, Winnipeg, Manitoba R3T 2N2, Canada

⁵ Canadian Ice Service, 719 Heron Road, Ottawa, Ontario K1A 0H3, Canada

INTRODUCTION

Ice bridges are rigid features that extend across relatively wide (tens of kilometres) channels (Sodhi, 1977; Rallabandi et al., 2017). Their formation is dependent on the channel width, ice shear strength, and the external stress applied by winds and currents (Hibler et al., 2006; Kubat et al., 2006; Rallabandi et al., 2017). Once in place the strength of an ice bridge increases thermodynamically, making the consolidated mass more stable (Hibler et al., 2006). While the bridge is in place it impedes ice drift through the channel, creating a latent heat polynya (area of open water and thin ice) beyond the pronounced arch of the bridge's leeward edge (Rallabandi et al., 2017). Eventually, either through an increase in external stress or weakening of the bridge through warming and melting of the ice, external forcing will overcome the strength of the bridge and cause it to collapse.

Perhaps the most well-studied ice bridges within the Canadian Arctic are those found in Nares Strait, Jones Sound, and Lancaster Sound, where the bridges preclude the advection of thick multiyear ice from the high Arctic and Canadian Arctic Archipelago (CAA) into northern Baffin Bay and thus maintain the North Water polynya (Kwok, 2005, 2007; Agnew et al., 2008; Kwok et al., 2010; Vincent, 2019; Kirillov et al., 2021). There are several other ice bridges that form annually across narrow interisland straits within the CAA that limit ice transport into the CAA from the Arctic Ocean (Howell et al., 2015) and maintain polynyas or flaw leads along their leeward edge throughout winter (Hannah et al., 2009). Within the Hudson Bay Marine Region (Foxye Basin, Hudson Bay, James Bay, and Hudson Strait), an ice bridge forms annually across Fury and Hecla Strait in northern Foxye Basin (Barber and Massom, 2007), while others form intermittently across Roes Welcome Sound (RWS), which separates Southampton Island from mainland Nunavut in northwestern Hudson Bay, between mainland Ontario and Akimiski Island in western James Bay (Taha et al., 2019), between mainland Quebec and Charlton Islands in eastern James Bay (Taha et al., 2019), and between the Belcher Islands and mainland Nunavik in southeastern Hudson Bay (Larouche and Galbraith, 1989; Fig. 1A).

Much attention has focused on the polynyas associated with the leeward sides of ice bridges rather than on the ice bridges themselves. Wherever bridges occur within striking distance of a community, Inuit and, in some cases, Cree community members report using them as a means of reaching areas that are otherwise inaccessible throughout winter. An Inuktitut term, *Nunniq*, describes a large, bridge-like, ice extent, particularly when places such as Cumberland Sound near Pangnirtung or Chorkbak Inlet near Kinngait (formerly Cape Dorset) freeze over (Laidler et al., 2008). In some instances, the ice bridges allowed Inuit who lived in island-based communities to get over to trading posts that had been established on the mainland. For example, there is a long history of Inuit from settlements

on the Belcher Islands in southeast Hudson Bay travelling across the ice bridge to trade at posts near the Great Whale River. Inuit from Sanikiluaq occasionally still travel across the ice bridge to visit friends in the communities of Kuujuarapik (Inuit) and Whapmagoostui (Cree). In James Bay, the ice bridges have been used by Cree to travel in the opposite direction, leaving behind busy mainland communities for better access to traditional activities, including hunting and gathering, on the islands.

In the RWS area (Fig. 1), Inuit from settlements on Southampton Island have crossed the ice bridge to the Nunavut mainland, especially the Wager Bay area (*Ukkusiksaliup Tariunga*; Inuit Heritage Trust, 2016), for generations. However, they know that the bridge only forms approximately every four years, meaning that the mainland is inaccessible to them during three of every four years. Many inhabitants of Coral Harbour, a settlement that formed in 1924 after a Hudson's Bay Company trading post was established, originally came from the Wager Bay-Naujaat area (T. Nester, pers. comm.). Thus, the ice bridge provides a useful travel route to access ancestral territories and to hunt caribou (*Rangifer tarandus*), wolves (*Canis lupus*), wolverine (*Gulo gulo*), and muskox (*Ovibos moschatus*) in the productive Wager Bay area on the mainland. Residents of Coral Harbour continue to use the ice bridge and refer to it locally as *nunniq*.

In order to know whether this important winter travel route between Southampton Island and the Nunavut mainland will persist into the future under a warming climate, it is essential to understand the mechanisms by which the bridge forms and why it only forms intermittently. In general, RWS is seasonally covered by sea ice from early November to late July (Andrews et al., 2018), with a narrow band of landfast ice forming along the coasts and a mobile ice pack occupying the central channel (Fig. 1). The general southward current and prevailing north-northwesterly winds advect ice southwards through the channel into Hudson Bay. Additionally, strong tides (daily tidal range of 3–8 m) maintain an extensive coastal flaw lead system along both sides of the channel, which typically presents as a recurrent polynya (Stirling and Cleator, 1981; Prinsenberg, 1986; Barber and Massom, 2007) that merges with the large polynya that forms along the ice edge in northwestern Hudson Bay (Landy et al., 2017; Bruneau et al., 2021). The combination of currents, winds and tides acting on a mobile ice pack within a narrow channel make for a dynamic ice cover that would be too dangerous to cross. Another potentially important factor in the formation of the ice bridge is the extreme cold of the area with average January and February temperatures of -30°C and occasional cold periods with temperatures dropping to -50°C .

In this paper, we first review the existing historical, scientific, and Inuit knowledge of the RWS ice bridge based on published materials and interviews conducted in the community of Coral Harbour during the last few years. Second, we expand on this knowledge base using a mix

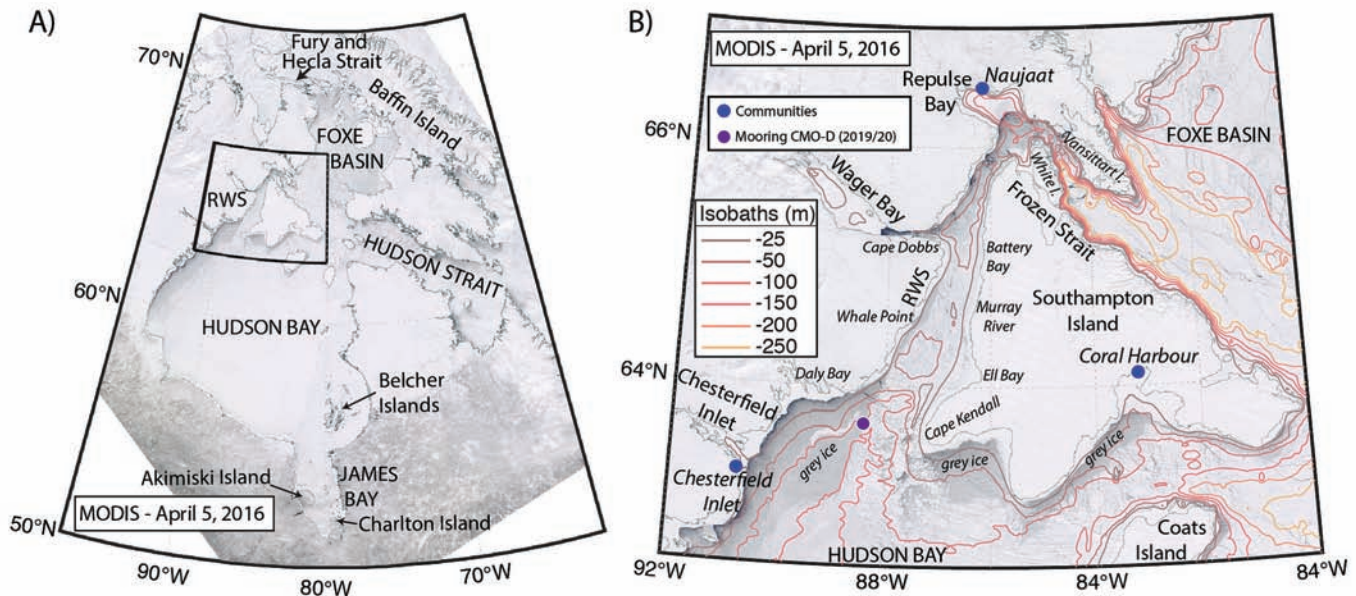


FIG. 1. A) Map of the Hudson Bay Marine Region, including Hudson Bay, James Bay, Hudson Strait and Foxe Basin. The locations of other ice bridges that form within the area are labeled. B) Map of the RWS study area in northwestern Hudson Bay. Bathymetry is from ETOPO1. Recurrent polynyas along the west coast of Hudson Bay, on the leeward side of Southampton Island, and near Repulse Bay are evident by the grey ice (darker shades of ice) and open water in these areas. The three Inuit communities in the RWS area are labeled with blue dots, and the purple dot shows the location of the CMO-D mooring in 2019–20. A MODIS image from 5 April 2016 is used for the background in both maps.

of remotely sensed, modelled, and reanalysis datasets to examine when and how the bridge forms and subsequently breaks up. The synthesis of the knowledge allows informed speculation as to why it only forms every four years. Finally, we discuss how a changing climate including warmer winters and shorter sea ice seasons in Hudson Bay may affect the formation of the ice bridge in the coming years with implications for Inuit who use it as a travel route.

SCIENTIFIC AND HISTORICAL KNOWLEDGE OF RWS AND THE ICE BRIDGE

Most of the scientific knowledge of RWS and the ice bridge arises indirectly from study of the polynya and associated biological communities. The polynya in RWS is commonly associated with the much larger polynya in western Hudson Bay (Landy et al., 2017; Bruneau et al., 2021), which is known to be highly productive (Barbedo et al., 2020; Pierrejean et al., 2020; Matthes et al., 2021). While there are no published in situ observations of productivity in RWS, strong tidal mixing is believed to generate hotspots of nutrient-rich surface waters particularly at the northern end of the sound (C.J. Mundy, pers. comm. 2021). Additionally, RWS is regarded as an important summer feeding area for narwhal (*Monodon monoceros*; Ross, 1974; Stirling and Cleator, 1981) and bowhead whales (*Balaena mysticetus*; Higdon and Ferguson, 2010), while several other animals such as ringed and bearded seals (*Pusa hispida* and *Erignathus barbatus*; DFO, 2020), eiders (*Somateria mollissima*; Prach et al., 1981), walrus (*Odobenus rosmarus*; DFO, 2020) and polar bears (*Ursus*

maritimus; Stirling and Cleator, 1981) overwinter in the polynyas around RWS. Because of its significance for marine wildlife and harvesting by Inuit, RWS has been identified as an ecologically and biologically significant area by Canada's Department of Fisheries and Oceans (DFO, 2011).

With a productive marine environment supported by polynyas and coastal flaw leads, the area around western Hudson Bay, RWS, Wager Bay, and Foxe Basin has a long history of inhabitation. The area around western Foxe Basin has been referred to as the “core area” of the Paleo-Inuit culture, which dates back to 2500 BC (Savelle and Dyke, 2014; Desjardins, 2020). In Wager Bay, Pre-Dorset peoples were present from 2000 to 800 BC, while Thule people inhabited this same area from the 11th century onward (Parks Canada, 2018). The Inuit group who lived on Southampton Island between 500 BC and ca. 1904 (the Sallirmiut or Sadlirmiut) were described as having “great permanency of settlements” relative to Inuit in other places (Price, 1970), which was perhaps because of the reliable local food supply.

In addition to marine mammals, Southampton Island has typically supported a caribou herd, which was a prime source of food for Inuit prior to European settlement on the island (Price, 1970). Following the establishment of the Hudson's Bay Company trading post on the island in 1924, the caribou population rapidly declined from overharvesting; by 1955, the caribou on Southampton Island had been eradicated (Parker, 1975; Campbell et al., 2020). Reintroduced to the island from Coats Island (*Appatuurjuaq*; Inuit Heritage Trust, 2016; Fig. 1B) in 1968 (Parker, 1975), the caribou population grew for 30 years

before eventually supporting a subsistence and commercial harvest in the 1990s (Nunavut Wildlife Management Board, 2020). The caribou population on Southampton Island peaked at 30,381 animals in 1997, but a combination of the reproductive disease *Brucellosis* and intensified harvest pressure from increased demand for caribou meat led to the herd's decline during the 2000s. The population fell to 7287 in 2013 but recovered somewhat to 12,297 in 2015 (COSEWIC, 2016). Typically, the Southampton Island herd is isolated on the island, with wide channels full of a dangerous mobile ice pack acting as a barrier to movement. However, Campbell et al. (2020) cite local knowledge that caribou occasionally immigrate across RWS over an ice bridge. Although Campbell et al. (2020) note that there is no documented evidence of a successful crossing, local knowledge and genetic analysis suggest that up to 5000 caribou may have immigrated across RWS during winter 2014. In particular, local hunters from Coral Harbour had observed “hundreds” of caribou tracks on the fast ice along the west coast of Southampton Island during winter 2014, although there was no specific mention of an ice bridge (Campbell et al., 2020). The immigration of caribou across the ice bridge was brought up once again during government consultations with the Coral Harbour Hunters and Trappers Organization in February 2020 (Nunavut Wildlife Management Board, 2020), with particular emphasis on its potential impact on the caribou population and therefore hunting quotas on Southampton Island.

Beyond Inuit habitation, the first European to explore RWS was Sir Thomas Button who travelled through the Sound in 1613 as he searched for the Northwest Passage. The Strait was subsequently mapped in 1631 by Luke Fox (also spelled Foxe, after whom Foxe Basin is named), who named it “Roes Welcome Sound” after the expedition's sponsor, Sir Thomas Roe. After the initial wave of explorers, American and British whalers harvested bowhead whales in RWS from 1860 to 1915, by which time the bowhead population had been hunted to near extinction (Ross, 1974). The first mention of the ice bridge that we have encountered in the historical written archives is a firsthand account from members of the Schwatka Expedition who were returning south on a whaling vessel during the first week of August 1879 and noted that the ice bridge was still present across RWS (Gilder, 1881:273): “We found plenty of ice in Daly Bay and the entrance to Roes Welcome Sound, the ice bridge still extending from near Whale Point to Southampton Island.” Daly Bay is located along the southwestern side of RWS (Fig. 1). This observation indicates that as far back as the late 19th century, the ice bridge was a known feature to the whalers and explorers of the area. Presumably the Pre-Dorset, Thule, and Inuit peoples who are known to have inhabited Wager Bay and Southampton Island had used the ice bridge for thousands of years prior to this period of European interest.

CONTEMPORARY LOCAL KNOWLEDGE OF RWS AND THE ICE BRIDGE

Inuit from the community of Coral Harbour (Salliq) on Southampton Island have used the ice bridge (*nunnig*) to cross RWS for generations. An Inuit knowledge holder interviewed for the Coral Harbour Nunavut Resource Inventory in February 2014 drew on a map the general area where the ice “sometimes freezes across to mainland and people go caribou hunting” and noted that the “last freeze up was 6 years ago” (i.e., 2008) (Government of Nunavut, 2014: Table 7). During more recent interviews, other knowledge holders said that the ice bridge forms approximately every four years. According to Troy Netser, “The ice bridge doesn't always happen. It happens what seems like once every four years.”

In terms of the factors that contribute to the formation of the bridge, community members said that it forms during mild winters and after full moons when the currents subside:

The colder the winter, the ice bridge won't be there because the ice freezes quicker and it's more brittle. When it's warmer out, the ice freezes slowly and bonds more, so it becomes harder for the current to break up the ice. That's when it freezes over and becomes an ice bridge.

(Troy Netser)

When the ice bridge is in place, hunters from Coral Harbour use it to cross RWS and hunt in the area around Wager Bay (Fig. 1). Historically, when the caribou herd on Southampton Island went down in size, hunters from Southampton Island crossed the ice bridge by dogsled to hunt caribou on the mainland. Hunters specifically relied on the ice bridge between 1955, when the caribou population was eradicated from overharvesting, and 1978, when hunters were able to begin harvesting caribou from the herd that had been reintroduced in 1968. Presently, with a stable caribou population on Southampton Island, hunters now mainly cross the bridge to hunt wolves, muskox, and wolverine. The pelts from these animals are either used to make parkas or sold and therefore represent an important resource and source of income for the community. Coral Harbour residents depend on a wide array of animals to supply their country food needs including caribou, geese, salmon, seal, and walrus. Ensuring access to and availability of country food continues to be an issue of importance and concern for the community (Government of Nunavut, 2014); when in place, the ice bridge expands access and ensures availability. Beyond Coral Harbour, people from Naujaat and Chesterfield Inlet know of the ice bridge but typically don't cross it.

In terms of crossing the bridge, some years the ice within the bridge is level “like a tabletop” (Troy Netser) and crossing it can take less than an hour. Conversely, during

other years the ice is very rough and it can take several days to cut a path through the pressure ridges.

The ridges can be as tall as houses, with chunks and chunks of ice piled up together. There's no way you could cross in that situation. I heard the bridge we had last year [2020] was like that, so there was no way to cross it.

(Troy Netser)

Community members said that pressure ridges are commonly present in the eastern edge of the bridge near the landfast ice edge along the west coast of Southampton Island, with smoother ice in the middle and western side of the bridge.

The ridges normally form where the solid ice [landfast ice], the old ice from fall freeze-up that is thicker and doesn't break as easily, meets the newer ice that forms and gets blown around, those are the pieces of ice that hit the solid ice and start piling up.

(Troy Netser)

METHODS

To build from the existing knowledge base about the ice bridge, we first used a combination of remote sensing platforms and ice charts to identify the years when the bridge formed and to determine the timing of bridge formation and breakup. Next, a mix of reanalysis and modelled data was used to examine the tidal forcing and atmospheric conditions around the periods of formation and breakup.

Remote Sensing of Sea Ice

Initially, ice charts from the Canadian Ice Service were used to identify years when the ice bridge had formed across RWS. Ice charts delineate different ice regimes with polygons that present sea ice concentration by stage of development using the World Meteorological Organization's egg code. Polygons are defined by expert manual interpretation of remotely sensed imagery and ship and airborne observations (Canadian Ice Service, 2005). Each polygon is assigned an egg code that describes the total ice concentration (tenths), partial ice concentration of up to three stages of development, and floe size (more information available in Tivy et al., 2011). Within the ice charts, the ice bridge is classified as a band of landfast sea ice (10-tenths concentration) and is clear from its concave arch along the southern edge (Fig. 2). Historically, the charts were developed with a view to supporting the summer shipping season and relied solely upon observations from ships and aircraft. The first ice chart for Hudson Bay was produced on 21 June 1971. From 1971 to 1979, ice charts for Hudson Bay were produced weekly or biweekly for the start

of the shipping season during June and July but were not produced prior to June. With the advancement of remote sensing technology, ice charts began to be produced during winter in 1980, although from 1980 to 2006, ice charts were only produced at monthly time scales during January, February, and March, biweekly during April and May, and weekly during June and July. From 2007 to 2011, ice charts were produced biweekly during January, February, and March, and weekly from April onward. Finally, since 2012, ice charts have been produced weekly throughout the year. Ultimately, 14 ice bridges were identified within the 50-year record of ice charts (Table 1; Fig. 3). However, due to the variability in the temporal coverage of the ice charts, it is impossible to narrow down the timing of formation and breakup. For instance, the ice bridges in 1973, 1976, and 1979 were present in the first chart produced in June, but it is unknown when these ice bridges formed. Ice bridges during 1984, 1990, 1994, 1996, and 1998 could be traced to their month of formation, but the timing could not be narrowed down beyond that. Similarly, the determination of breakup timing was limited to a 1- to 2-week window.

Optical imagery from the Landsat series of satellites and the Moderate Resolution Imaging Spectrometer (MODIS) were also used to look for ice bridges in RWS and narrow down the timing of bridge formation and breakup. Using the United States Geological Survey's Global Visualization viewer (GloVis online viewing platform; <https://glovis.usgs.gov>), archived Landsat imagery from the Multispectral Scanner on Landsat 1-5 (1972–92; 80 m spatial resolution) and the Thematic Mapper on Landsat 4-5 (1982–2012; 30 m spatial resolution) were examined for bridges. One limitation to the Landsat platforms was the availability of imagery, which was generally only available biweekly from March onwards. MODIS was launched in 2000 and provides over 20 years of daily optical imagery at a spatial resolution of 250 m over RWS. MODIS images were accessed through the National Aeronautics and Space Administration's Earth Observing System Data and Information System (EOSDIS) Worldview platform (<https://worldview.earthdata.nasa.gov>). The improved temporal coverage of MODIS also revealed the temporary formation of three bridges in 2008, 2011, and 2014, which persisted only for a few days, and we define as unstable bridges (Table 1; Fig. 3). This discovery suggests that additional unstable bridges may have formed prior to the start of the MODIS time series in March 2000 but were not observed due to the lower temporal resolution provided by the earlier satellite platforms. MODIS also revealed the formation of an ice bridge north of Southampton Island across Frozen Strait during winter 2003 and 2014, which we will discuss further below.

While MODIS provides an excellent time series of observations, it is impeded by clouds, which can be fairly prevalent in the area of RWS and thereby limit our ability to narrow down the timing of formation or breakup. In the instances of excessive cloud cover, radar imagery from either RADARSAT-1 (1998–2013), RADARSAT-2 (2007–present), or Sentinel-1 (2014–present) was used

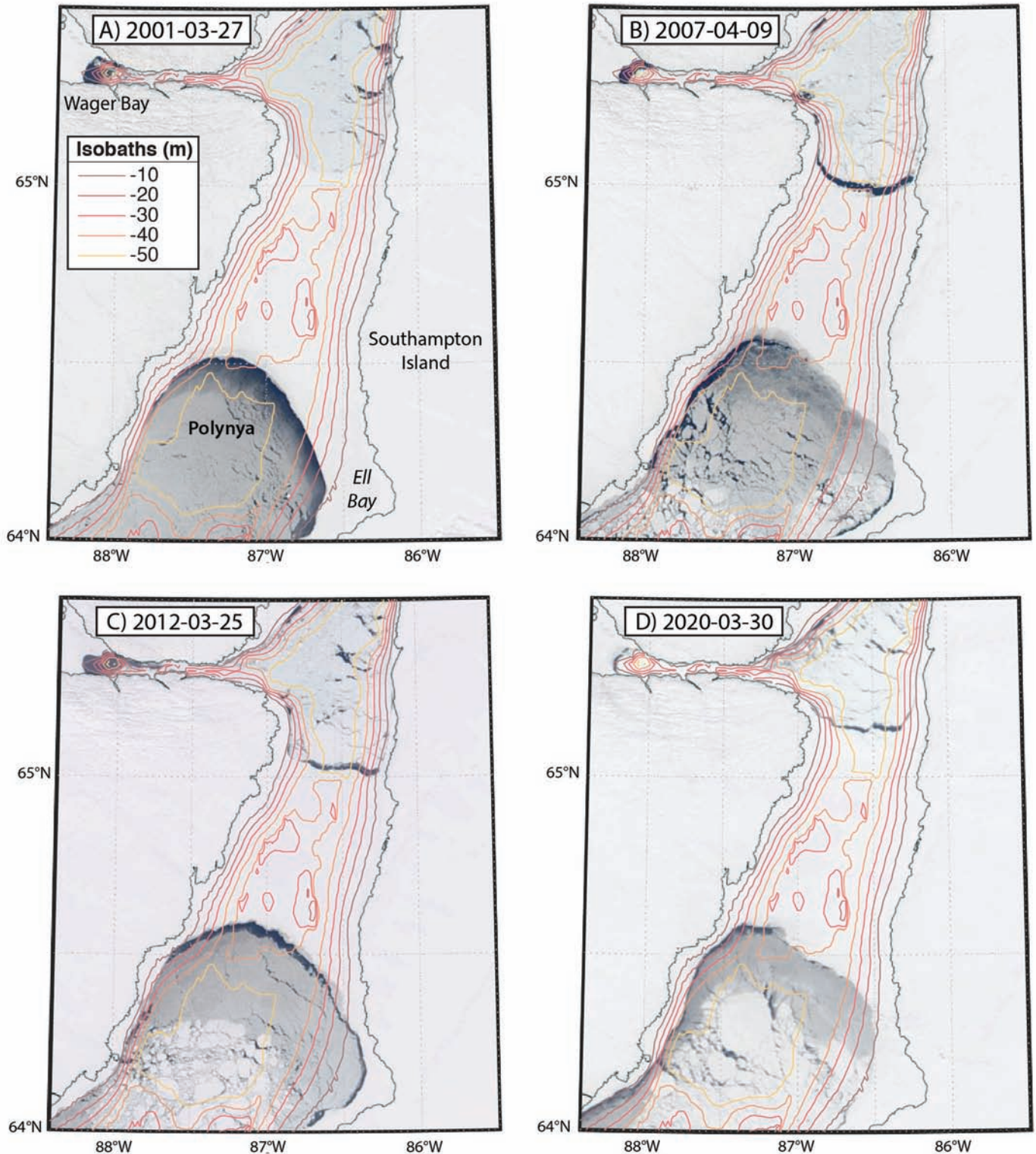


FIG. 2. MODIS imagery of the RWS ice bridge during winter A) 2001, B) 2007, C) 2012, and D) 2020. Isobaths down to 50 m are presented.

to see through the clouds and narrow down the timing of formation and breakup (Table 1). However, the temporal coverage of radar imagery also varies considerably, so in some instances a combination of ice charts, MODIS, and radar imagery were used to narrow down the timing of the formation and breakup of the ice bridge. Ultimately,

the exact date of formation was determined for the seven most recent bridges, while the exact date of breakup was determined for three of these bridges and narrowed down to 2–4 days for the remaining four (Table 1; Fig. 3).

Given that there are no in situ measurements of the ice characteristics within the bridges, radar imagery provides

TABLE 1. Dates of ice bridge formation and breakup and the observation used to identify the stable and unstable ice bridges. Note that for some bridges the exact date could not be determined so a window of a month or a few days is provided.

Year	Formation	Observation	Breakup	Observation
Stable bridges:				
1973	Prior to 20 March	Landsat	Mid-July	Ice chart
1975	10 March–14 April	Landsat	25 April–16 June	Landsat
1976	Prior to February 26	Landsat	Mid-July	Ice chart
1979	Prior to February 18	Landsat	Late June	Ice chart
1984	February	Ice chart	Late June	Ice chart
1985	Prior to February 28	Landsat	14–21 June	Landsat
1990	February	Ice chart	Mid-July	Ice chart
1994	January	Ice chart	Late June	Ice chart
1996	January	Ice chart	Early July	Ice chart
1998	January	Ice chart	Late June	Ice chart
2001	5 January	MODIS	14 June (MODIS) – 18 June (Ice chart)	MODIS & ice chart
2007	11 March	Radarsat-1	1 July	MODIS
2012	4 March	Radarsat-1 and -2	11–14 June	MODIS
2020	8 January	Sentinel-1	5–7 July	MODIS
Unstable bridges:				
2008	15 March	MODIS	23 March	MODIS
2011	13 March	MODIS	16–17 March	MODIS
2014	7 March	MODIS	9 March	MODIS

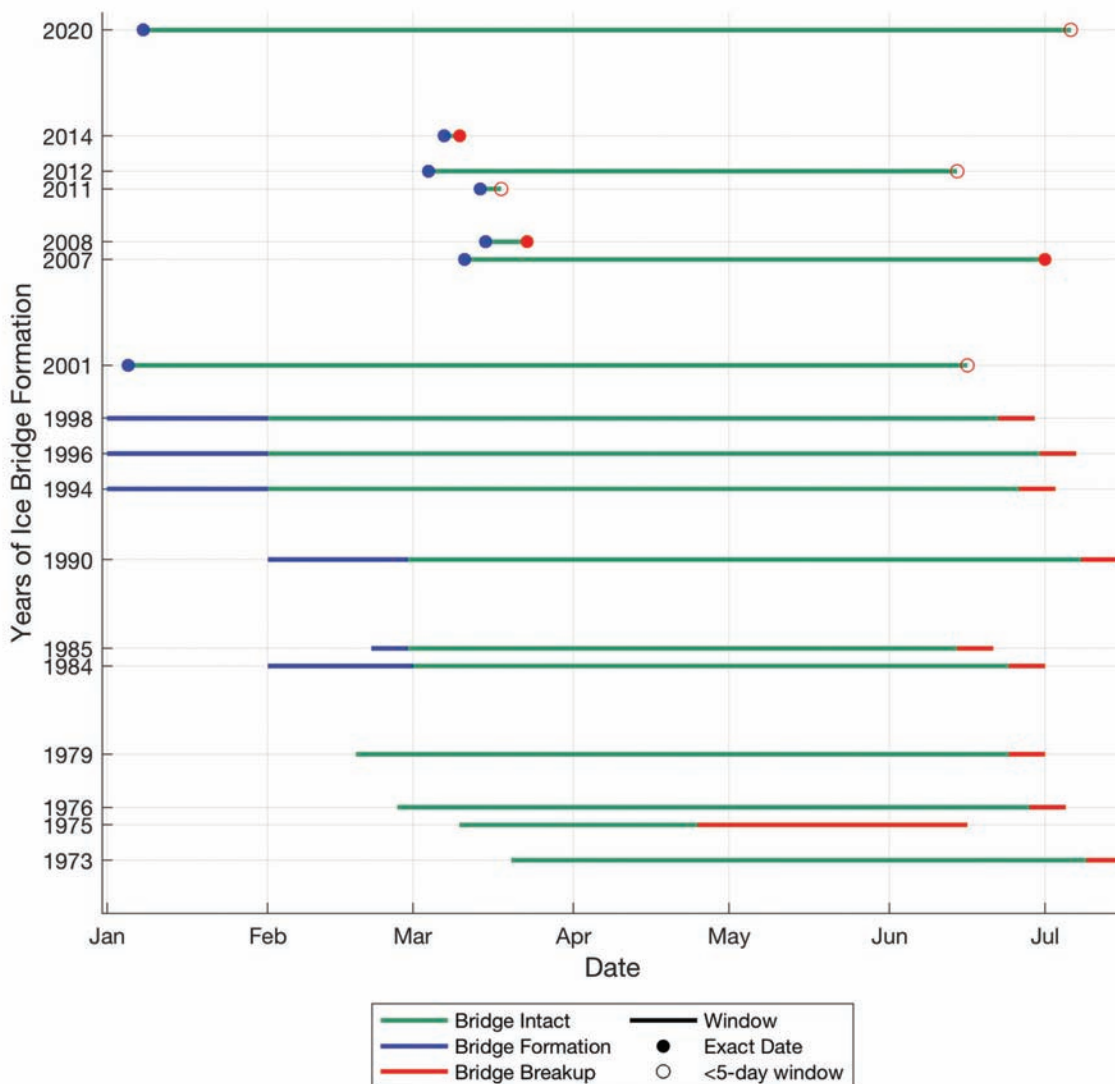


FIG. 3. Timing of the formation and breakup of the RWS ice bridge from 1971 to 2020. Blue denotes the period of formation and red denotes the period of breakup. Windows of formation and breakup are denoted by lines, while exact dates of formation and breakup are denoted by dots.

context on the composition and structure of the RWS bridges in 1998, 2001, 2012, and 2020, and the Frozen Strait bridges in 2003 and 2014. From its higher resolution and interaction with the surface of the ice, radar provides information on the ice roughness and identifies large individual ice floes within the bridge.

In terms of ice thickness within the bridge, there are no known recorded observations. However, ICESat-2 (Ice, Cloud, Land Elevation Satellite; Kwok et al., 2019), which was launched in fall 2018, provides estimates of sea ice freeboard within the bridge that formed during winter 2020. ICESat-2 houses a laser altimeter (Advanced Topographic Laser Altimeter System; ATLAS) that counts individual photos to measure elevation along three pairs of strong and weak beams. Within this study, we only consider the strong beams. In ice-covered waters, ICESat-2 provides estimates of freeboard by defining the mean sea surface height from leads within the ice pack and then determining the elevation of the sea ice or snow surface relative to the sea surface. Because there are no leads within the bridge itself, the sea surface height was linearly interpolated across the length of the bridge from leads beyond the northern and southern arches. The sea ice height dataset (ATL07/L3A) acquired from the National Snow and Ice Data Center provides elevations for sea ice and leads at ~15 m along-track resolution for the three strong beams (Kwok et al., 2020).

Atmospheric and Oceanographic Forcing

Based on the timing of formation and breakup determined above, 6-hourly fields of 2 m air temperature (T_{2m}), 10 m winds, and sea level pressure from ERA-5 (Copernicus Climate Change Service (C3S), 2017) were used to examine atmospheric forcing over RWS around the periods of formation and breakup. The time series of T_{2m} was used to calculate a sliding 5-day sum of freezing degree days (FDD), where $FDD = -1.8^{\circ}\text{C} - T_{2m}$, with -1.8°C being the freezing point of seawater. Note that because we used 6-hourly data, the FDD from each 6-hour point was divided by four as it represents the FDD during one-quarter of the day. Also, the 5-day sum is calculated for the final day of the 5-day period, that way the FDD on the day of formation represents the five days prior to formation. Overall, FDD indicates how cold it has been during those five days and could be used to estimate thermodynamic ice growth (H_{ice}) following the equation $H_{ice} = 1.33 * FDD0.58$ (Lebedev, 1938). Both along-channel (210°T) and across-channel (120°T) projections of wind speed were calculated and smoothed to a running 72-hour mean. The mean and standard deviation of these running means were then calculated to provide context on the typical forcing around bridge formation and breakup. Seasonal trends in 2 m air temperatures over RWS were calculated from ERA-5 for the 1979 to 2020 period and tested for significance.

In terms of oceanographic forcing, an hourly time series of modelled tidal amplitude at the centre of the southern

end of RWS (64.75°N , 86.87°W) was extracted from the WebTide Tidal Prediction Model v0.7.1 that is run through the Bedford Institute of Oceanography (BIO, 2020). More information on the tidal model for Hudson Bay is available from Saucier et al. (2004). In the absence of observational data on current velocities, the tidal phases are the only reliable parameter characterizing the relative intensity of water dynamics in the Strait. Generally, the regional large-scale thermohaline circulation governs the mean southward flow and this flow can be suggested to be the same if ice bridges form under the same wind forcing. If so, the tidal flow is the main source of high frequency variability, which is of interest in terms of bridge formation. In situ observations of tidal velocities from the CMO-D mooring deployed south of RWS in winter 2019–20 (Fig. 1) revealed relatively low variability in tidal currents between neap and spring tide during winter (2 and 5 cm/s, respectively). However, this mooring was deployed south of the channel, and currents may be confined and therefore amplified within the channel.

A similar analysis of atmospheric and tidal forcing was done for the ice bridges that formed across Frozen Strait in 2003 and 2014. Tides were extracted from the middle of Frozen Strait (65.54°N , 84.14°W), while both across-channel (160°T) and along-channel (70°T) projections of wind speed were calculated.

Bathymetry

We retrieved bathymetry data of RWS and Frozen Strait from the ETOPO1 Global Relief Model (Amante and Eakins, 2009) at 1-arc minute resolution (Fig. 1). A subset of the data product was retrieved from the National Oceanic and Atmospheric Administration's (NOAA) National Centers for Environmental Information. Additionally, the Canadian Hydrographic Services nautical chart for the study area was referred to for added detail on the bathymetry of these channels.

RESULTS

During the 50 winters from 1971 to 2020, 14 ice bridges formed across RWS and offered a stable platform for Inuit to travel from Southampton Island to the mainland area around Wager Bay (Fig. 3; Table 1). An additional three unstable bridges were detected to have formed temporarily during winter 2008, 2011, and 2014, although they quickly collapsed; additional unstable ice bridges prior to 2000 may have gone undetected. Although the bridges formed sporadically over the last 50 years, on average, a stable ice bridge has formed across RWS once every four years, which agrees with the local knowledge of the bridge.

The location and size of the bridge shows minimal variability between years, with well-defined northern and southern arches that extend from the coastal band of landfast ice (Fig. 2). The northern arch spans approximately

30 km from Cape Dobbs at the southern end of the entrance to Wager Bay to an area between Battery Bay and the Murray River on the west coast of Southampton Island. The southern arch spans approximately 60 km from Whale Point on the mainland to the northern end of Ell Bay on the west side of Southampton Island, although in 2001 the bridge extended to the southern end of Ell Bay (Fig. 2A). Typically, the central length of the bridge is about 50 km, with the bridge approximately covering between 2300 km² (2012) and 3100 km² (2001). Although it is unclear if any portion of the ice bridge is grounded, it is important to note that the bridge does form over an area with multiple shoals that are shallower than 30 m, with one particular area in the southeastern portion of the bridge shallower than 20 m (Fig. 2). Markham (1986) suggested that the landfast ice edge in the nearby Foxe Basin stabilizes around the 20 m isobath, indicating that ice in this area is dynamically thick enough to become grounded at the 20 m depth and supports the notion that a portion of the bridge may be grounded. Once the bridge is established it prevents the typical southward drift of sea ice through RWS, causing pack ice to be trapped in the confined area north of the bridge and leading to the formation of a wind-driven latent heat polynya off the southern arch (Fig. 2). Additionally, the formation of a tidal-driven flaw lead is evident twice per day beyond the northern arch as the ebb tide advects the mobile ice northward (Fig. 2B).

Ice Bridge Formation

Focusing on the seven recent ice bridges for which the exact date of formation (Day 0) can be determined (2001, 2007, 2008, 2011, 2012, 2014, and 2020), we examined the atmospheric conditions and tidal forcing around the timing of formation (Fig. 4). In terms of tidal forcing, five of the seven bridges formed within two days of neap tide, when the daily tidal range at the entrance to RWS was below 5 m (Fig. 4a). The two bridges that formed beyond this 2-day window (2008 and 2014) were unstable and collapsed within a few days of formation.

Across all seven bridge formation events, the average air temperature began declining 10 days prior to formation, falling below -29°C on the day of formation and dropping below -30°C two days after formation (Fig. 4b). The reduction in air temperature around bridge formation is reflected in an increase in FDD from a typical value of approximately 120 during the preceding month, to 140 on the day of formation (Fig. 4c). The two bridges that formed under slightly warmer conditions (-20°C and -25°C) were the same unstable bridges that temporarily formed beyond the 2-day window around neap tide in 2008 and 2014. For the stable ice bridges, air temperatures generally remained below -25°C and FDD remained above 140 for up to 10 days after formation (Fig. 4b and 4c).

Although winds were highly variable, on average the along-channel wind speeds peaked at 4 m/s 12 days prior to formation before declining to 0 m/s on the day

of formation (Fig. 4d; note the exaggerated scale for the mean and standard deviation of winds). Conversely the average across-channel wind speed reached a seasonal minimum 14 days prior to formation and increased steadily to a seasonal peak of 4 m/s two days prior to formation (Fig. 4e). The transition from high along-channel winds and calm across-channel winds approximately two weeks prior to bridge formation to calm along-channel winds and strong across channel winds during formation indicates a rotation of surface winds from the prevailing northerly flow to a more west-northwesterly flow around the time of formation (Fig. 5). This change affects ice motion within the channel, which instead of being advected southward into Hudson Bay will instead be advected eastward against Southampton Island. Beyond the magnitude of wind speed, we also see a reduction in the standard deviation (red line in Fig. 4d and e) of both the along- and across-channel wind speeds around formation, indicating winds were more stable and less variable while the bridge formed. Following bridge formation, along-channel wind speeds remained less than 5 m/s for up to six days, while across-channel wind speeds generally maintained a western heading and remained between 2 and 3 m/s for the 10 days following formation (Fig. 4). Overall, these seven formation events are characterized by a prolonged period of very cold air temperatures around neap tide, which coincides with a rotation of winds from the prevailing northerly direction to more west-northwesterly flow and an overall reduction in the along-channel wind speed.

Radar imagery of the ice bridge in 1998, 2001, 2012, and 2020 revealed that the ice bridge is predominantly composed of rougher pack ice (Fig. 6; rougher pack ice has higher backscatter and is therefore presented as lighter pixels). However, within the western side of these four bridges there is a band of smooth ice (lower backscatter and therefore darker pixels) located between the previous landfast ice edge and the rougher pack ice. In 1998, this smooth area was very pronounced, extending through the full western side of the bridge and having a maximum width of 15 km. In 2001 and 2020, the area of smooth ice was much narrower (5–10 km wide) but still extended through much of the western side of the bridge. In 2012, the area of smooth ice was confined to the southwestern corner of the bridge and reached a maximum width of approximately 2 km. This band of new ice likely formed after the rotation to west-northwesterly winds compressed the existing ice pack against Southampton Island and exposed an area of open water along the landfast ice edge of the western channel where new ice formed rapidly under cold air temperatures. Specifically, this ice would have had to grow thick enough during the cold and calm period that typically follows formation to maintain a stable bridge once along-channel winds began to increase. From the peak in across-channel winds two days prior to formation through to the increase in along channel winds six days after formation, the 5-day FDD remained around 140. Therefore, during this 8-day period, we estimate 24 cm of ice growth in the western end of the bridge.

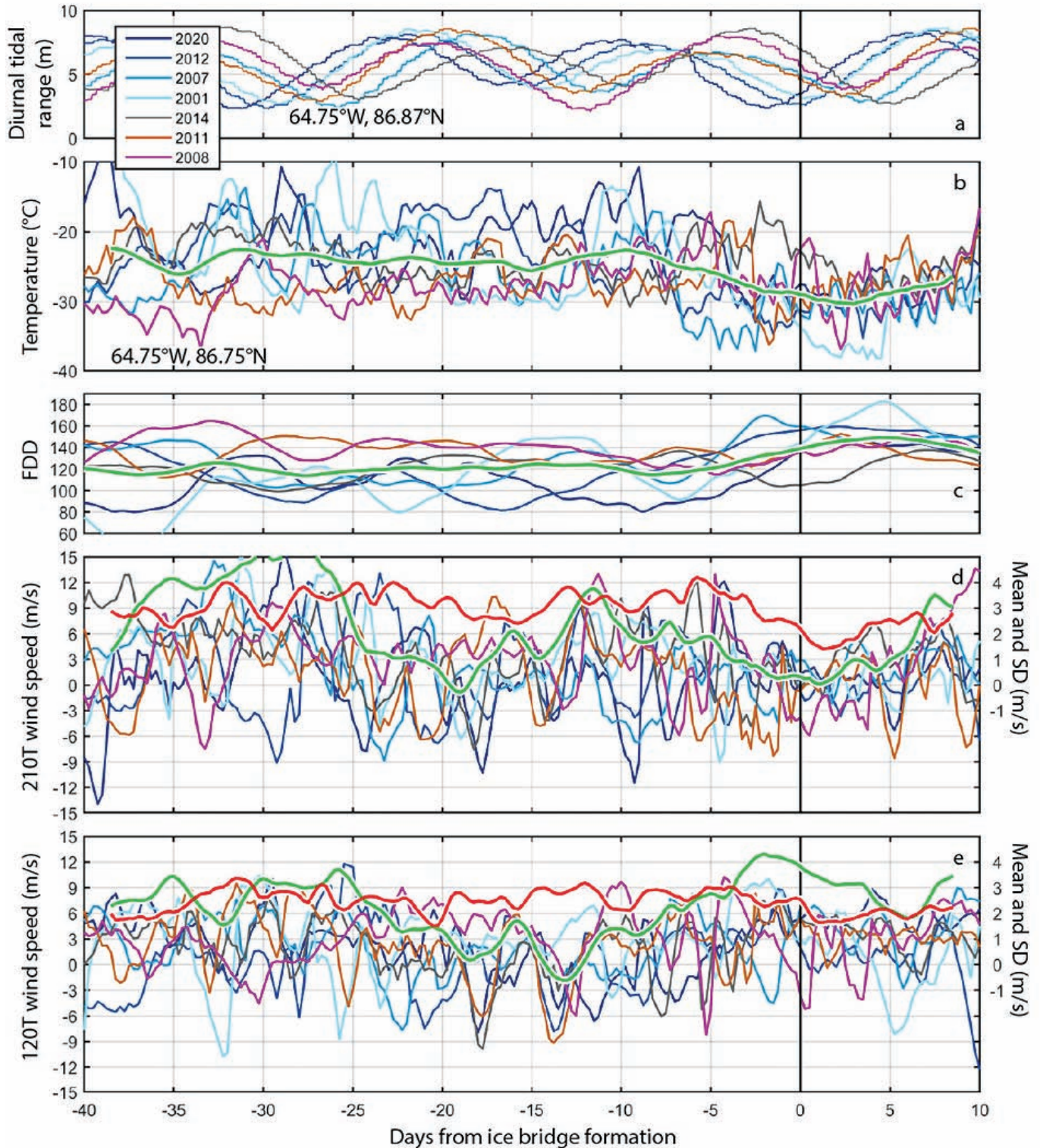


FIG. 4. Time series of a) daily tidal range (m), b) 6 h surface air temperature (°C), c) 5-day moving sum of Freezing Degree Days, d) along-channel (T210) and e) across-channel (T120) wind speeds (m/s) for the period prior to the day of ice arch formation (Day 0) during the last 7 ice bridge events. Air temperatures and winds were smoothed with a 72 h moving mean. The mean (green) and standard deviation (red) of the time series are presented for the atmospheric variables. The mean and standard deviation of the winds have been scaled by three and correspond to the y-axis on the right side of the figure.

In terms of ice thickness, an ICESat-2 transect along the middle of the bridge on 13 June 2020 revealed that a majority of the bridge was composed of a relatively homogenous ice cover with a modal freeboard of 0.16 m and

an average freeboard of 0.30 m (Fig. 7A). An area of thicker ice with a mean freeboard of 0.55 m was located beyond the original edge of the bridge that formed in January (black line in Fig. 7) and can be traced to the northward extension

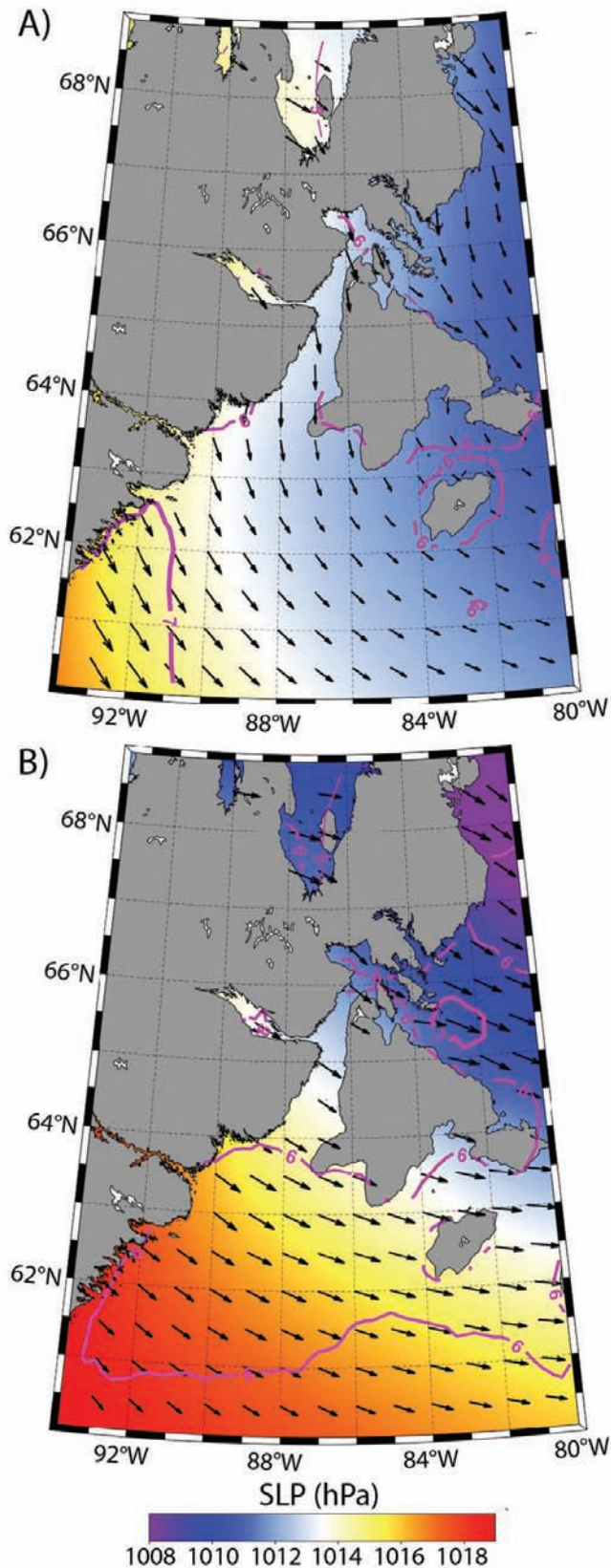


FIG. 5. Mean sea level pressure (SLP) and surface winds averaged over the study area from A) the 30 days between 35 days and five days prior to formation, and B) the three days during formation from two days prior to formation to two days after formation. Speed isotachs are shown in magenta contours.

of the bridge during a storm in March. This ice was thicker as it had been dynamically deformed in the confined area beyond the northern arch before it eventually adhered to the bridge in March. Surface melt became evident one day after the ICESat-2 transect; therefore, using the simplified assumption that there was no snow on top of the ice, we estimate a mean ice thickness of 1.73 m within the original bridge and 3.24 m in the northern end of the bridge (with assumed ice density of 930 kg/m^3 ; note these estimates of total thickness are overestimations due to the assumption of no snow). A transect across the bridge on 2 April 2020 revealed a pronounced reduction in freeboard from east to west across the bridge, before once again highlighting the area of thicker ice along the northern end of the bridge (Fig. 7B). Within the original portion of the bridge, there is a clear decrease in sea ice freeboard from approximately 0.4 m in the east to 0.15 m in the west. This decrease supports the proposed process of bridge formation, in which westerly winds cause the thicker existing ice cover to converge in the eastern channel while new ice forms rapidly in the western channel to lock in the bridge. Freeboard estimates greater than 1 m are present in both transects and highlight the presence of heavily deformed pieces of ice and very thick ridges within the bridge. These features may potentially be thick enough to become grounded on the shallow shoal in the eastern side of the channel (Fig. 2) and stabilize the bridge.

Ice Bridge Breakup

Once the ice pack has consolidated and the bridge has formed, it either stabilizes and persists through spring until it breaks up between mid-June and mid-July, or it doesn't stabilize (2008, 2011, 2014) and breaks up within a few days of formation (Fig. 3). There is no middle ground for the bridge; it either lasts for a few days or four to six months.

In terms of the unstable bridges, two of the three (2008 and 2011) broke up under strong winds, while one bridge (2014) never fully consolidated and broke up two days after the northern and southern ice arches became evident. The 2008 bridge was the most unusual. While the 5-day running FDD was 140 around formation, the temperature on the day of formation was relatively warm (-20°C). Additionally, it formed during a temporary reversal to southeasterly winds (negative values in Fig. 4d and 4e). The bridge formed slightly farther south than the stable bridges, and although cold air temperatures followed three days after formation ($< -35^\circ\text{C}$), the bridge gradually collapsed over a few days until eventually an increase in northerly along-channel winds ($> 6 \text{ m/s}$ seven days after formation; Fig. 4d) caused the bridge to collapse during the following day. The 2011 bridge formed much farther south than other years and may have therefore been inherently weaker because of the greater width of its southern arch. Regardless, the bridge broke up five days after formation during a period of strong southerly along-channel winds ($\sim 5 \text{ m/s}$; orange line in Fig. 4c). Following the collapse of an unstable bridge it

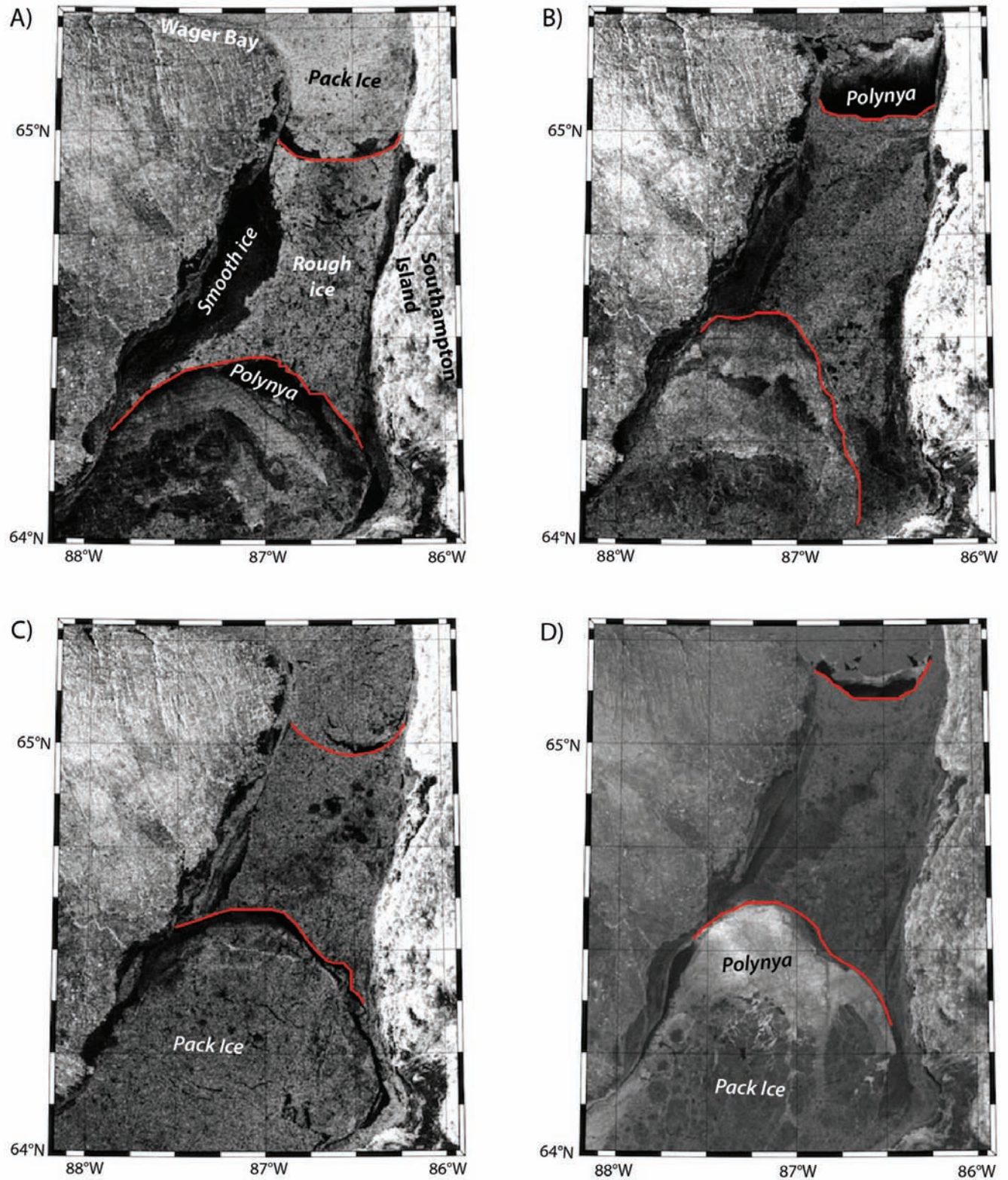


FIG. 6. RADARSAT-1 and -2 images of the ice arch from A) 1 February 1998, B) 2 February 2001, C) 17 March 2012, and D) 22 March 2020. The northern and southern arches are outlined in red.

would be possible for another bridge (stable or unstable) to form within the Strait, however this was not observed and is unlikely given the conditions that need to align for a bridge to form.

Stable bridges remain intact through spring and typically break up between mid-June and early July (Table 1; Fig. 3). By this time air temperatures are above 0°C and surface melt features (e.g., melt ponds and surface flooding) are

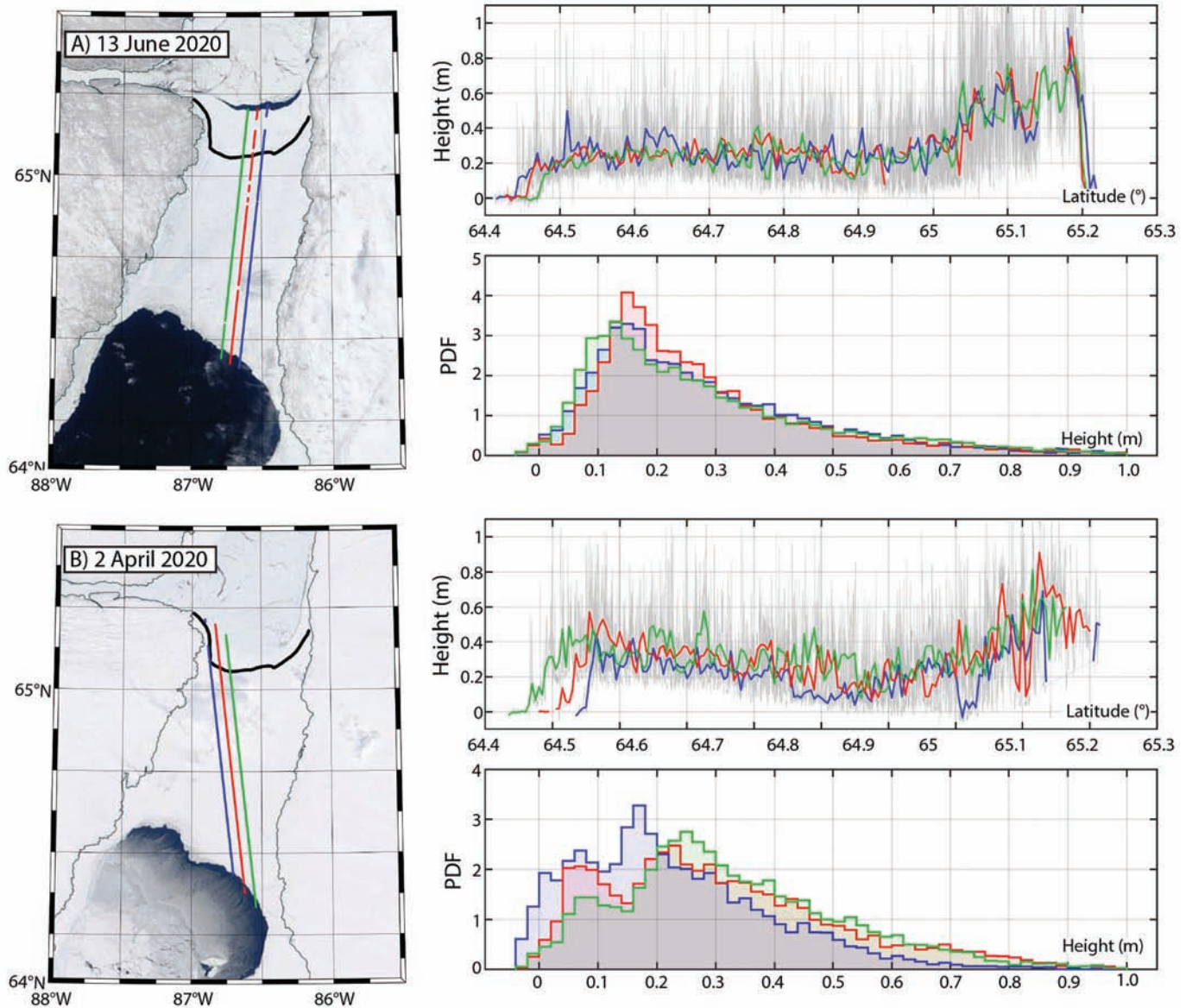


FIG. 7. ICESat-2 transects of sea ice freeboard (ATL07) across the RWS ice bridge on A) 13 June 2020 and B) 2 April 2020. For each transect, a map of the three strong beams is overlaid on a MODIS image of the ice bridge on the same day, while the plots on the right show sea ice freeboard plotted against latitude as well as the probability density function (PDF) of sea ice freeboard for each strong beam.

present across the bridge (Fig. 8). In particular, the band of thinner, smooth ice that formed on the western side of the bridge is evident in MODIS imagery as a band of grey ice or flooded ice just prior to breakup (Fig. 8). In terms of forcing around the time of breakup there appears to be two different mechanisms. First, the ice bridges of 2001 and 2012 (blue and yellow, respectively, in Fig. 9) broke up in mid-June around neap tide, while air temperatures were just above 0°C , and during periods of pronounced northerly winds ($> 10\text{ m/s}$). Conversely, the ice bridges of 2007 and 2020 (green and red, respectively, in Fig. 9) broke up two weeks later in early July around spring tide, following periods of warm air temperatures ($> 10^{\circ}\text{C}$) and under calm winds. The first mechanism reflects the dynamic breakup of the bridge as strong northerly winds exceed the strength of the melting bridge and cause it to collapse. The second

mechanism reveals less dynamic forcing, but greater warming and therefore further weakening of the bridge, which breaks up as either greater tidal forcing or the slight reversal to southerly winds disrupts the bridge and causes it to collapse. Given the unpredictable nature of winds, it is advisable that once temperatures reach 0°C and the melt season begins, the ice bridge should no longer be used for crossing RWS.

DISCUSSION

The Intermittent Nature of the Ice Bridge

Both local Inuit knowledge from the community of Coral Harbour and the 50-year record of satellite imagery

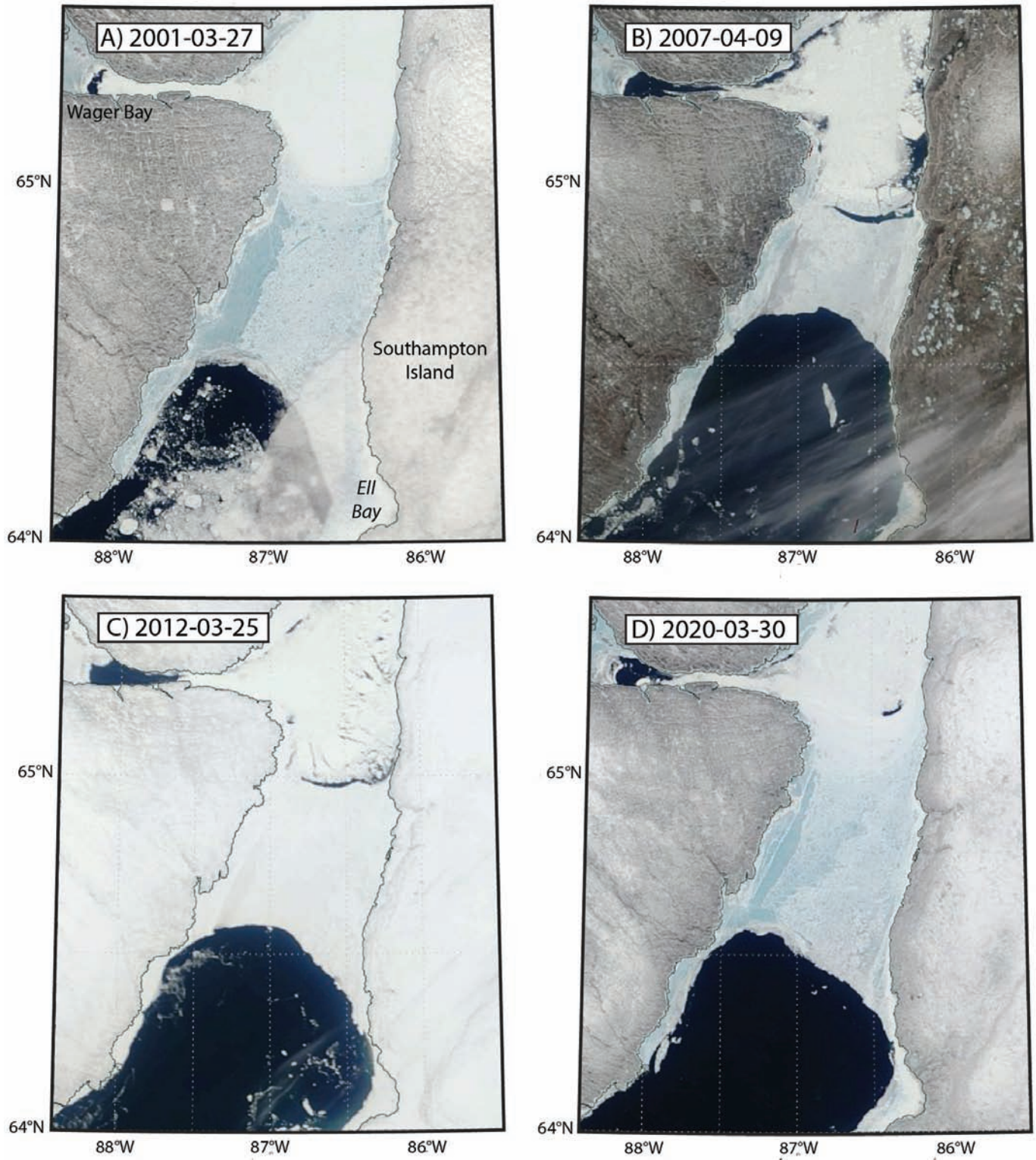


FIG. 8. MODIS images of the ice bridge just prior to breakup in June A) 2001, B) 2007, C) 2012, and D) 2020.

and ice charts confirm that on average an ice bridge forms across RWS in northwestern Hudson Bay every four years. However, the timing between bridges is highly variable. The bridge has only formed during back-to-back years twice (1975 and 1976, and 1984 and 1985), while between 1994 and 1998 the bridge formed every other year. The

longest period between stable bridges is eight years (2012–20; Fig. 3; Table 1), though six- and five-year gaps have also been observed (1979–84, 1985–90, 2001–07). Overall, on average a stable bridge forms every four years, though the bridge may form during consecutive years, or it may not form for up to eight years.

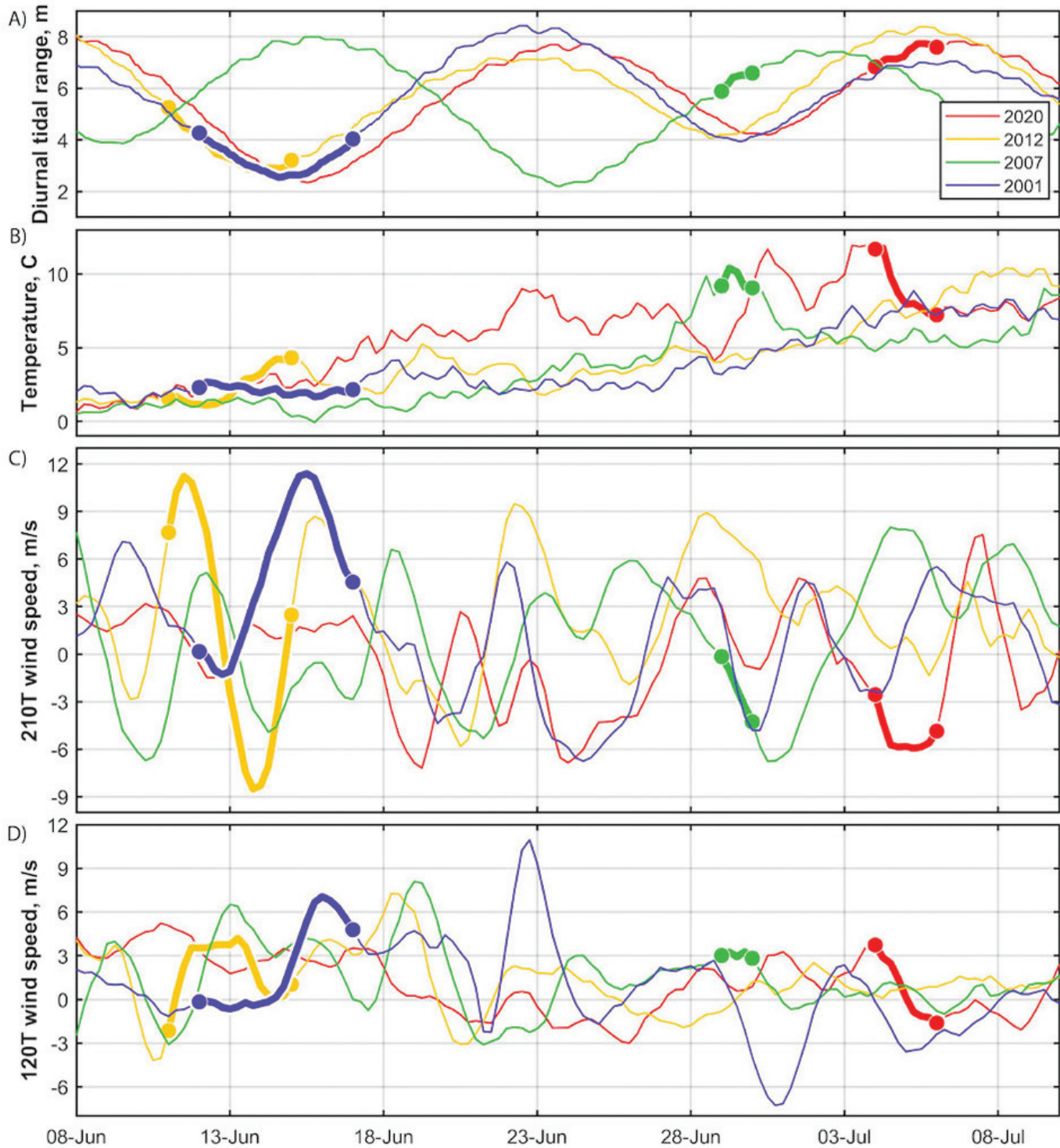


FIG. 9. Time series of the A) daily tidal range (m), B) air temperature (°C), C) along-channel and D) across-channel winds (m/s) around the time of bridge breakup in 2001, 2007, 2012, and 2020. The thick lines highlight the timing of breakup, and the dots show the start and end of the window (Table 1).

Typically, the ice bridge forms between January and March and breaks up between June and early July, providing a stable transportation route for Inuit for up to six months. Through determining the exact date of formation of the seven most recent ice bridges and examining the tidal forcing and atmospheric conditions around these events, we determined that the bridge generally forms around neap

tide (diurnal tidal range < 5 m) during prolonged periods of cold air temperatures (< -25°C and 5-day FDD > 140) and while the prevailing winds have rotated from the typical northerly, along-channel flow to a west-northwesterly, across-channel flow. The across-channel winds compress the existing ice pack against Southampton Island, while relatively small tidal forcing and along-channel winds make

for a relatively immobilized ice cover that coalesces under cold air temperatures, which is similar to the process that facilitates the formation of the ice bridge in Nares Strait (Kirillov et al., 2021). An estimated 24 cm of new ice rapidly forms on the western side of the channel and locks the bridge in place. Location is also important. Generally, the bridge forms south of the entrance to Wager Bay and north of Ell Bay. If the arch forms farther south where the sound widens near Ell Bay (Fig. 1), it may be too weak to stabilize. There were two instances in the satellite record (2008 and 2011) when bridges failed to stabilize likely because they had formed too far south. An increase in along-channel winds shortly after formation may also cause the bridge to collapse before it stabilizes. However, if winds remain calm and cold temperatures prevail beyond approximately seven days after formation, the bridge will stabilize and become strong enough to oppose external forcing until it begins to melt and eventually collapses between mid-June and early July. While this describes the mechanism for the formation and breakup of an ice bridge across RWS, it leaves us wondering why the bridge only forms every four years on average. RWS is characterized by a long cold winter, cyclical tides, and continuously varying winds, yet these conditions seem to only align between January and March every four years. In the following discussion, we examine several factors that may impact the formation of the ice bridge and explain its intermittent nature.

An important factor for the consolidation of an ice bridge is the existence of an ice cover that is thick enough and therefore strong enough to oppose external forcing once it has consolidated (Sodhi, 1977; Kubat et al., 2006; Rallabandi et al., 2017; Kirillov et al., 2021). If the ice cover is too thin it may consolidate, but it will simply be too weak to oppose external forcing and break up once wind speeds increase. While we have estimated 24 cm of new ice growth during an 8-day window from the peak in across-channel winds to the return of strong along-channel winds, a majority of the bridge comprises much thicker and stronger sea ice. Without in situ observations of ice thickness within RWS around the timing of formation, it is impossible to know the ice thickness threshold required for bridge formation. A 54-year record of landfast ice thickness collected through a community-based monitoring program in Coral Harbour revealed an average landfast ice thickness of 80–120 cm near the community between January and March (Candlish et al., 2019; Environment and Climate Change Canada, 2020). However, these measurements were collected on level landfast ice, whereas the ice pack within RWS is a dynamic ice cover that is typically heavily fractured by the combination of strong winds and high tides forcing the ice cover within a narrow channel. Generally, the prevailing northerly winds (Fig. 5a) advect the ice cover southward through RWS towards Hudson Bay, although across-channel winds and tides drive an extensive flaw lead along the landfast ice edge on both sides of the channel. While new ice forms within the flaw leads, these

leads are also the site of considerable sea ice deformation as the mobile ice pack is forced against the landfast ice edge, creating very thick pieces of ice (e.g., Barber et al., 2021). Radar imagery reveals that the bridges were predominantly composed of roughened ice, with large floes present amongst the ridges and rubble fields (Fig. 6). Heavily deformed floes within the ice pack, such as those observed in southern Hudson Bay by Barber et al. (2021), may contribute to the stabilization of the bridge by becoming grounded on the shallow shoal near the southeastern end of the bridge, though with a depth of 20 m this would require an extremely thick piece of sea ice. While thick deformed ice makes the ice pack stronger and increases the likelihood of grounded ice stabilizing the bridge, if deformation has made the ice pack too rough, as it was in 2020, it may be impassable. Given that freeze-up typically occurs in RWS between late October and mid-November (Andrews et al., 2018), it seems that the ice cover requires at least two months of growth, both thermodynamic and dynamic, before the ice cover is thick enough for the bridge to potentially form. However, between 1979 and 2020 there was no relationship between the timing of freeze-up and bridge formation, which highlights the importance of specific atmospheric conditions and tidal forcing in the consolidation of the existing ice pack and formation of an ice bridge across RWS.

Focusing on the window of formation from January to March, we examined the variability of tides, air temperatures, and winds during this period. In terms of tides, five of the seven recent bridges, including all four of the stable bridges, formed around neap tide while the daily tidal range was below 5 m. Within the window of formation, from 2000 to 2020, the daily tidal range was below 5 m on 31.6% of the days or approximately one-third of the time. In terms of air temperatures, the 1979–2020 mean during the window of formation was -28.3°C , which is similar to the mean air temperature on the day of formation (Fig. 4b). However, bridge formation is characterized by a prolonged cold period when the 5-day FDD exceeds 140, which is equivalent to 24 cm of thermodynamic ice growth. This threshold of FDD was only surpassed on 5% of the days during the period of formation between 2000 and 2020. In terms of wind speed, the average along- and across-channel wind speeds were 1.8 and -2.0 m/s, indicative of the prevailing north-northwesterly winds over RWS during winter (Fig. 5a). However, between 2000 and 2020 the winds rotated to a dominant easterly heading with an across-channel wind speed exceeding 4 m/s during only 5.8% of the time. Additionally, following this rotation, along-channel winds must remain calm while the bridge stabilizes. From 2000 to 2020, along-channel wind speeds were only quiescent (-0.5 to 0.5 m/s) 6.4% of the time and rarely for a prolonged period.

Ultimately, the intermittent nature of the ice bridge is due to the rare co-occurrence of a prolonged period of very cold air temperatures (5%), tidal ranges below 5 m (31%), and the relatively rare rotation from northwesterly

to westerly winds within the 6 h reanalysis data (5.8%). Additionally, if these three factors align and a bridge does form, it needs to form in the narrow part of the channel between Wager Bay and Ell Bay, and along-channel winds need to remain relatively calm during the following week. If the first three factors do align and the ice consolidates but these last two factors aren't met, the bridge will likely break up before it stabilizes.

With these general conditions around bridge formation in mind, we can look at the time series of tides, air temperatures, FDD, and along- and across-channel winds during each winter and speculate on why the bridge may not have formed during other years. Focusing on examples from 2003, 2010, and 2018 (Figs. 10, 11, 12), it is clear that the co-occurrence of the different factors is rare given their temporal variability. During 2003, a prolonged cold period from mid-February to early March may have increased the chance of bridge formation, but part of this period was characterized by spring tide, while along-channel winds were highly variable and calm across-channel winds indicate the winds never rotated. In 2010, the air temperature never fell below -30°C and FDD never surpassed 140, indicating that winter 2010 may have been too warm for the ice bridge to form. Additionally, winds were extremely variable during winter 2010, with frequent reversals to southeasterly winds that advect the ice pack away from Southampton Island and prevent it from consolidating. A two-week cold snap in February 2018 aligned with neap tide, though during this time the across-channel winds flipped to an easterly heading. From MODIS imagery, it is clear that the ice in RWS was immobile for a few days during this time, yet the ice was never advected against Southampton Island, and when the across-channel winds flipped to an easterly heading, a large flaw lead opened up along the east side of the channel. Ultimately, bridges did not form during these years, which highlights how rare it is that all of the factors align and lead to the formation of the bridge. It must also be noted that this list of factors is not exhaustive and other factors such as ice thickness, ridge depth, and current speeds also likely contribute to the formation of the bridge.

The fact that the bridge forms during prolonged cold periods does not agree with the local knowledge that the bridge forms during mild winters. However, the period around bridge formation may be perceived as being relatively warm because of the occurrence of calm winds, particularly in an area where strong north-northwesterly winds can dramatically amplify the perceived temperature by increasing the wind chill. Additionally, the rotation of winds during bridge formation is the result of higher pressure over RWS (Fig. 5), which generally makes for sunnier conditions that can also reduce the perceived temperature. Furthermore, the presence of a vast polynya south of the bridge may also affect the perception of temperature on Southampton Island, though warm moist air from the polynya would typically be advected to the southeast over Cape Kendall (*Kipkaq*) and towards central Hudson Bay (Fig. 5).

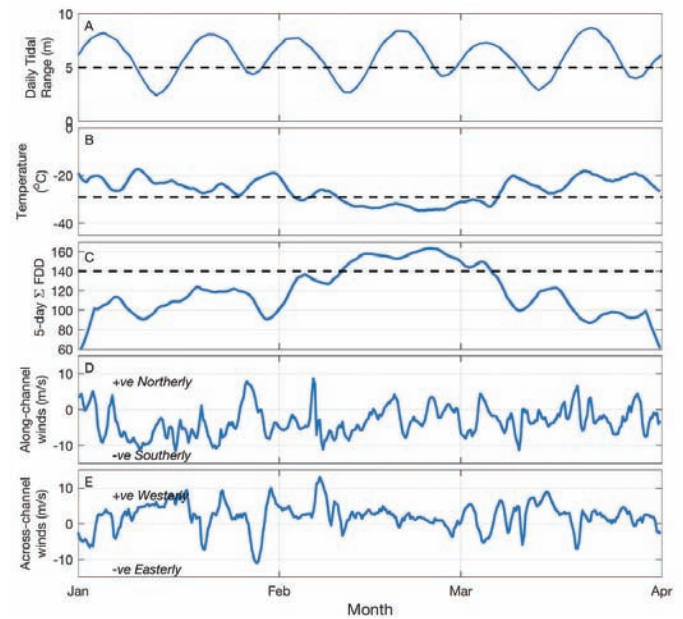


FIG. 10. Tidal and atmospheric forcing time series during the winter of 2003 when the ice bridge did not form in RWS. The figure shows A) tidal amplitude (m), B) 2 m air temperature ($^{\circ}\text{C}$), C) running 5-day sum of FDD, and D) along-channel and E) across-channel wind speeds (m/s) in RWS from January to April. Thresholds defined in the text are provided as dashed lines.

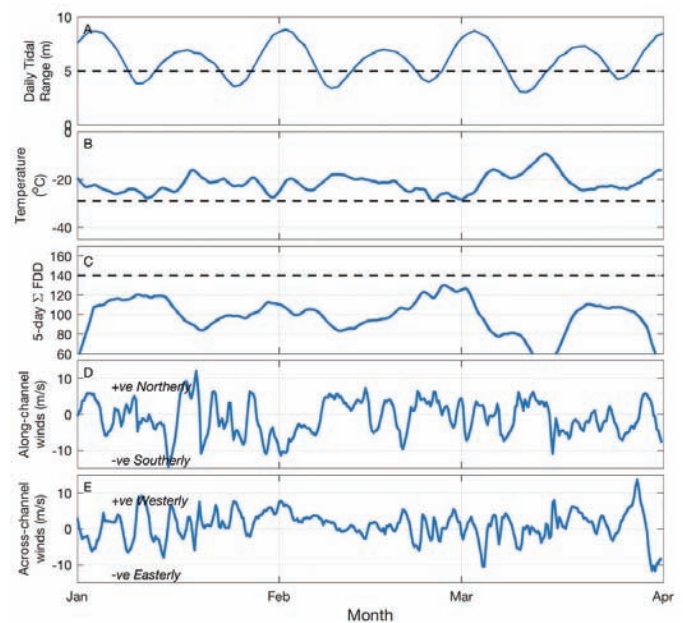


FIG. 11. Tidal and atmospheric forcing time series during the winter of 2010 when the ice bridge did not form in RWS. Variables shown as in Figure 10.

Implications of Climate Change

Given that formation of the bridge depends on a suitably thick ice cover in RWS, cold air temperatures, and the magnitude and orientation of surface winds, it is reasonable to expect that climate change and the transition towards warmer temperatures and shorter sea ice seasons will affect the ice bridge and therefore Inuit who use it as a travel route. Shifts in wind patterns may already be underway.

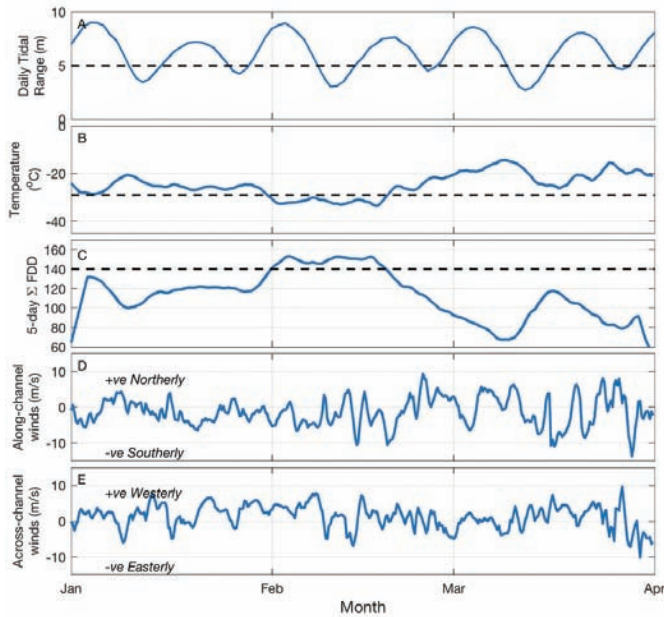


FIG. 12. Tidal and atmospheric forcing time series during the winter of 2018 when the ice bridge did not form in RWS. Variables shown as in Figure 10.

The Inuit knowledge study conducted for Ukkusiksalik National Park (Ukkusiksalik Inuit Working Group et al., 2013) described several changes in wind patterns in the RWS area. An 81-year-old Elder, who grew up at Wager Bay, noticed that the wind used to come from the northwest but this has changed to more winds from the north.

[I]t does not seem to get windy from the northwest. When I was growing up the wind was always coming from the northwest. We hardly had any winds from the southeast and the north but nowadays it seems to be more windy from the north...

(Robert Tatty – 2009 Interview, Inuit Knowledge Project [original in Inuktitut])

According to the Ukkusiksalik Inuit Working Group et al. (2013), “many Elders spoke of how the wind has increased in frequency and in intensity compared to the past. The most reported change to the wind was that nowadays there are fewer calm days.” Calm winds are critical for bridge formation as they allow the ice to remain consolidated and coalesce.

In addition to shifts in wind, Elders from the RWS area who contributed to the Inuit Knowledge Study also observed warming. In the 2012 Inuit Knowledge Workshop, Jerome Tattuinee noted that “The sun is much hotter” (Inuit Knowledge Project [original in Inuktitut]).

Atmospheric reanalysis indicated a significant ($p < 0.05$) trend of $+0.6^{\circ}\text{C}/\text{decade}$ in mean air temperatures during the window of formation (January to March) between 1979 and 2020. Although air temperatures today remain cold during winter, a persistent warming trend during the window of formation will lead to a thinner ice pack within RWS, slower

coalescence of the compressed ice pack, and slower formation of new ice in the western bridge. In particular, underlying the positive trend in air temperatures is a considerable reduction in the number of very cold days ($< -30^{\circ}\text{C}$), which are typical around bridge formation. The online interactive Climate Atlas of Canada (www.climateatlas.ca) shows the number of very cold ($< -30^{\circ}\text{C}$) days per year over RWS (region: Yellow Bluff) is predicted to decrease by approximately one-third, from an average of 82 between 1979 and 2005 to 50 between 2021 and 2050 under high carbon emissions scenarios. Collectively these changes may require a longer period of calm winds and cold air temperatures for the bridge to stabilize, making it less likely in a given year that the bridge does stabilize and perhaps reducing how often the bridge forms in coming years.

Beyond warming during winter, more pronounced warming has occurred during fall ($+1.2^{\circ}\text{C}/\text{decade}$ from 1979 to 2020; $p < 0.05$; October to December), leading to delayed freeze-up within RWS (Andrews et al., 2018). Although ice bridge formation was found to not be directly related to the date of freeze-up, delayed freeze-up does generally lead to a thinner ice pack during winter and may push back the start of the window of formation.

Similarly, warming air temperatures during spring ($+0.4^{\circ}\text{C}/\text{decade}$ from 1979 to 2020; $p < 0.05$; April to June) will force the end of the window of formation earlier in the year; if a bridge does form, warmer air temperatures during spring will likely advance the onset of surface melt and thereby encourage earlier breakup of the ice bridge. Although there is no trend underlying the breakup of the 14 ice bridges that formed between 1970 and 2020 (Fig. 3), they did break up notably earlier than the historic observation of the ice bridge being in place through to the first week of August 1879 (Gilder, 1881). Beyond the bridge, warming during spring has led to significant trends towards earlier breakup of the ice pack in RWS (Andrews et al., 2018) and landfast ice around the nearby communities of Coral Harbour and Chesterfield Inlet (Cooley et al., 2020). Ultimately, a warmer atmosphere, particularly a reduction in very cold days, and a shorter sea ice season with later freeze-up and earlier breakup may reduce the likelihood of the ice bridge forming and persisting through spring when local Inuit hunters use it to travel to Wager Bay.

Wildlife and the Ice Bridge

While Inuit have crossed the ice bridge for generations, it is unknown if wildlife crosses the bridge or how the polynya and flaw lead that form along the edges of the bridge affect marine wildlife. Recently, Campbell et al. (2020) cited local knowledge that caribou do cross the ice bridge across RWS, but noted that no immigration had been documented. However, as noted earlier in the discussion of scientific and historical knowledge of the RWS ice bridge, Campbell et al. (2020) combined local knowledge and genetic analysis to propose that approximately 5000 caribou immigrated across RWS onto Southampton Island between May 2013 and 2015,

during which time the caribou population on the island nearly doubled. This immigration likely occurred during late winter 2014 when local hunters reported observations of “hundreds” of caribou tracks along the fast ice on the west side of Southampton Island. Campbell et al. (2020) did not specifically mention an ice bridge; however, our analysis reveals that an unstable ice bridge formed across RWS between 7 and 9 March 2014 (Table 1). Although short in duration, this bridge may have facilitated the immigration event proposed by Campbell et al. (2020). Furthermore, if caribou cross the bridge, it seems likely that wolves and wolverines, which are known to hunt caribou, may follow them across the bridge. Similarly polar bears may cross the bridge, though they would likely stick to the edges where seals may be present within the polynya and flaw lead.

In terms of its effect on the marine environment, the ice bridge switches the ice cover from a dynamic mobile ice pack with narrow leads to a vast solid ice cover (> 2400 km²) with pronounced edges and a large polynya. These two different states may be advantageous for different species. In the North Water polynya, interannual variability in ice density and amount of open water is known to affect the whales and seals differently, with a larger polynya allowing whales access to a larger proportion of the region but providing fewer opportunities for walrus and seals to haul out on ice (Heide-Jørgensen et al., 2013). While there is very limited information about whale usage of RWS during winter, Richard et al. (1990) previously suggested that the western Hudson Bay beluga (*Delphinapterus leucas*) population overwintered in the leads in RWS. Aerial surveys during March 1982 did not reveal any beluga in RWS, and it has since been determined that the western Hudson Bay beluga population overwinters in Hudson Strait, though local sources have reported beluga sightings during winter along the ice edge around RWS (Richard et al., 1990). Bowhead whales are known to congregate in RWS, Repulse Bay, and Frozen Strait during summer, though the conservative estimates of their population vary from just 35 to 75 individuals (Cosens and Innes, 2000; Frasier et al., 2020). It is not known when bowhead return to RWS because of a lack of tagging data during this time of year (S. Ferguson, pers. comm. 2021), though killer whales (*Orcinus orca*) have been sighted at the floe edge near Repulse Bay in the spring (June) (Ferguson et al., 2010), which implies some of their main prey species (bowhead and narwhal) are already present in the area. This finding indicates that the ice bridge across RWS may overlap with the return of whales to the area and therefore may affect their migration.

During spring, migrating seabirds use the polynya in northwestern Hudson Bay to stage and forage as they move into their breeding colonies (DFO, 2020); the presence of a larger polynya due to the bridge may promote these activities. Additionally, the larger open water area during ice-bridge years would also presumably result in stronger upwelling of deep nutrient-rich waters, supporting higher productivity in western Hudson Bay (Matthes et al., 2021)

and increasing food supply to benthos, which is consistent with the predicted benthic hot spot immediately south of RWS (Pierrejean et al., 2020). The biological impact of the bridge and the large polynya associated with its formation are areas for future research.

Frozen Strait Ice Bridge

In addition to the ice bridges that formed across RWS, our analysis of MODIS satellite imagery revealed that an ice bridge formed across Frozen Strait (*Qiqiqtaaluuplu*; Inuit Heritage Trust, 2016) during winter 2003 and 2014 (Fig. 13A and 13B). Note that there was no ice bridge across RWS in 2003 and only an unstable, short-lived ice bridge across RWS in 2014, so the two bridges don't correspond to each other. Frozen Strait is a narrow but deep channel that runs from Repulse Bay to the southwestern corner of Foxe Basin and is part of the deep channel that runs across southern Foxe Basin (Fig. 1; Campbell, 1964; Defossez et al., 2008). The Strait connects Foxe Basin to RWS and onto northern Hudson Bay. Southampton and White Islands comprise the southern shore, while Vansittart Island and part of Melville Peninsula comprise the northern shore of the Strait (Fig. 1). Inuit from Coral Harbour know of the ice bridge across Frozen Strait and have crossed it to travel to Naujaat but say that they typically avoid it as stronger currents make for a rougher ice cover that is more difficult to cross and less stable.

The ice bridge in Frozen Strait doesn't happen as often as the one to the west, but people do cross it. It's closer to Naujaat. Although I don't think it is as safe as the one to the west because there is so much current in Frozen Strait. I don't think it is as stable.

(Troy Netser)

In 2003, the ice bridge across Frozen Strait formed on 11 February and broke up on 31 May, while in 2014 it formed between 26 and 31 January and broke up on 4 June. During both instances the bridge formed at the eastern end of Frozen Strait, with its western edge located from White Island (*Qiqiqtaaluk*; Inuit Heritage Trust, 2016) to Vansittart Island (*Nagjuttuuq*; Inuit Heritage Trust, 2016) (17 km), and its eastern edge spanning the mouth of Frozen Strait from Cape Comfort (*Isatialuk*; Inuit Heritage Trust, 2016) on Southampton Island to the southeast corner of Vansittart Island (50 km; Fig. 13). The central length of the Frozen Strait ice bridge was approximately 70 km during both years, and the bridge covered an approximate area of 2500 km².

In terms of forcing during the formation of the ice bridge in Frozen Strait, both bridges formed during cold periods (< -20°C) and around neap tide (Fig. 14). In terms of winds, typically northwesterly winds blow over Frozen Strait (Fig. 5), advecting the ice pack out of the Strait into Foxe Basin. However, both bridges formed during periods of relatively calm northeasterly winds that likely stopped the advection of sea ice out of Frozen Strait and instead

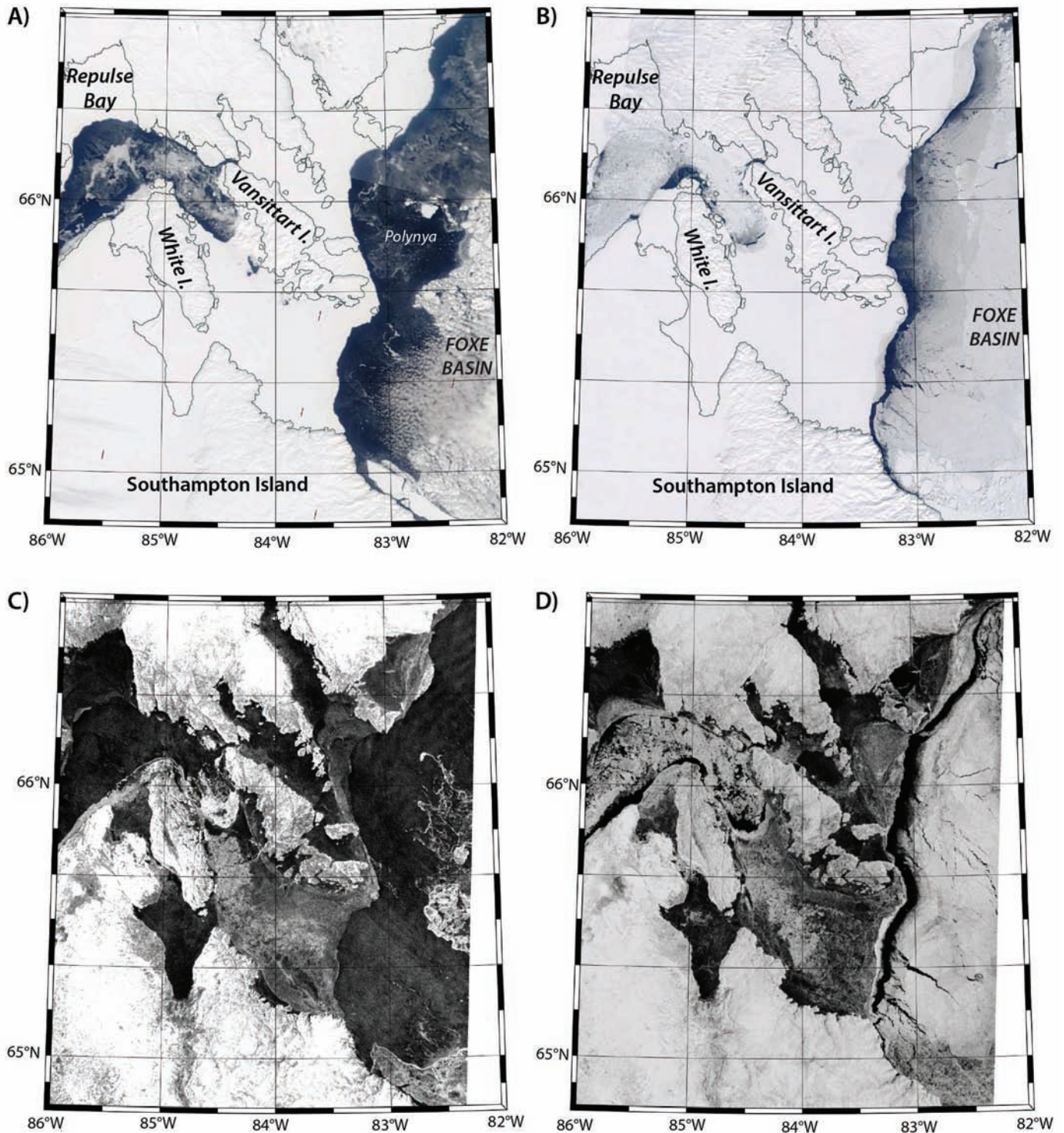


FIG. 13. MODIS imagery of the ice bridge across Frozen Strait on A) 13 May 2003 and B) 17 March 2014, and RADARSAT-1 imagery of the ice bridge across Frozen Strait on C) 13 May 2003 and D) 17 March 2014.

compressed the ice pack back up Frozen Strait against Southampton and White Islands (Fig. 14). This process is confirmed by RADARSAT imagery (Fig. 13C and 13D), which reveals roughened pack ice (brighter pixels) in the western and southern portions of the bridge against White Island and Southampton Island and smoother ice (darker pixels) near Vansittart Island on the northeast portion of the

bridges. Thus, similar to the RWS ice bridge, the occurrence of particular wind conditions timed with the neap tide seem to be necessary for ice bridge formation in Frozen Strait. One difference between the bridge in RWS and the bridge in Frozen Strait is that Frozen Strait is a much deeper channel (< 250 m in the center) with no shallow shoals (Fig. 1) hence there is no grounded ice to stabilize the bridge.

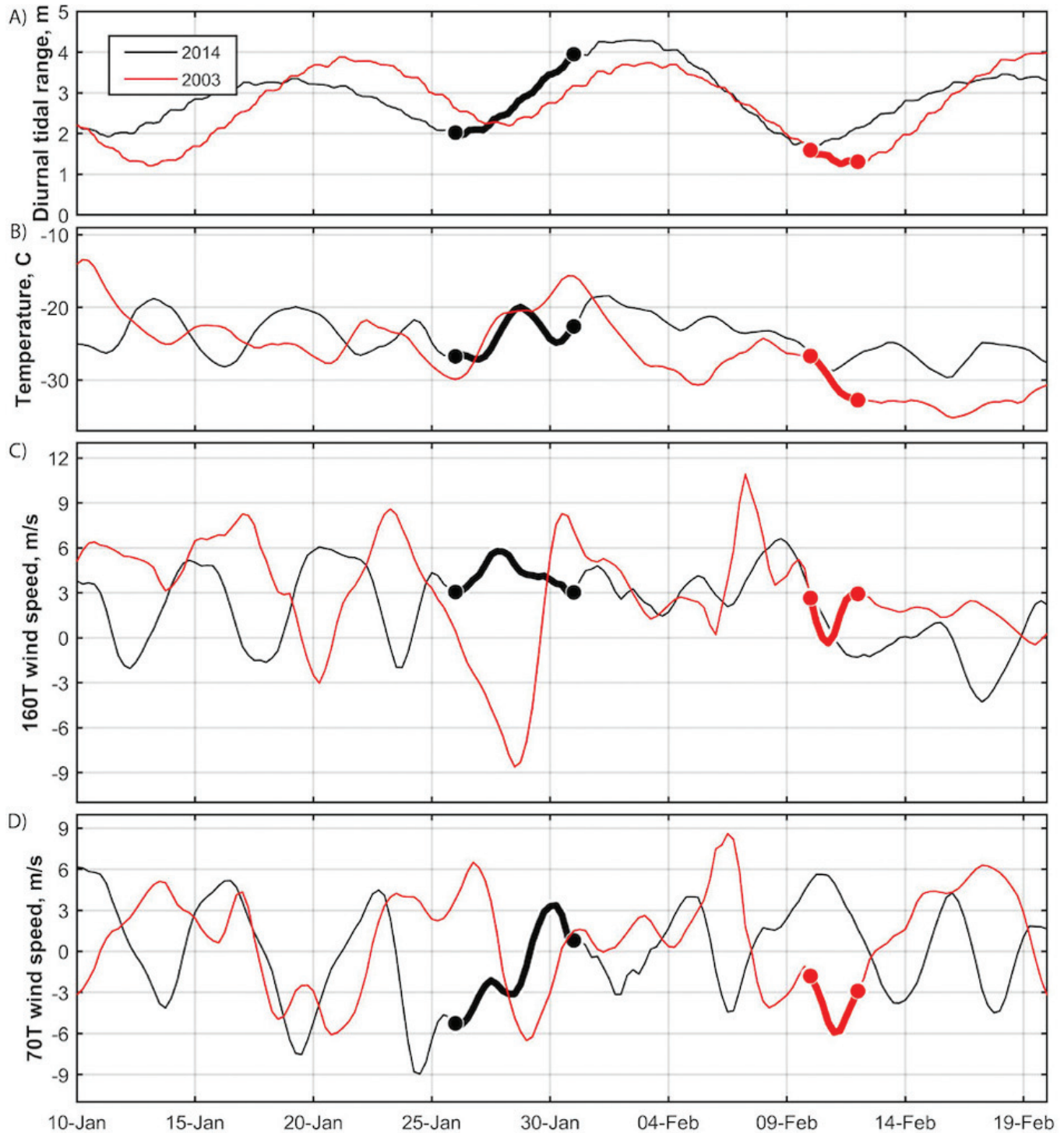


FIG. 14. Time series of the A) daily tidal range (m), B) air temperature (°C), C) along-channel and D) across-channel winds (m/s) around the time of bridge formation in Frozen Strait in 2003 and 2014. The thick lines highlight the timing of formation and the dots show the start and end of the window.

Both of the observed bridges in Frozen Strait began breaking apart along the western and eastern edges in mid-May, and eventually collapsed at the end of May or in early June. Neither of the bridges displayed any signs of surface melt prior to their collapse as air temperatures had yet to remain above 0°C for prolonged periods (Fig. 15). There was a peak (> 10 m/s) in northwesterly winds during the

final collapse of the bridge in 2014 and fairly steady (~5 m/s) northwesterly winds during the final collapse in 2003 (Fig. 15). The fact that both bridges in Frozen Strait collapsed earlier than the bridges across RWS and gradually collapsed over a two-week period before surface melt had begun indicates that the ice bridge across Frozen Strait is inherently less stable, which may explain why it forms much less often.

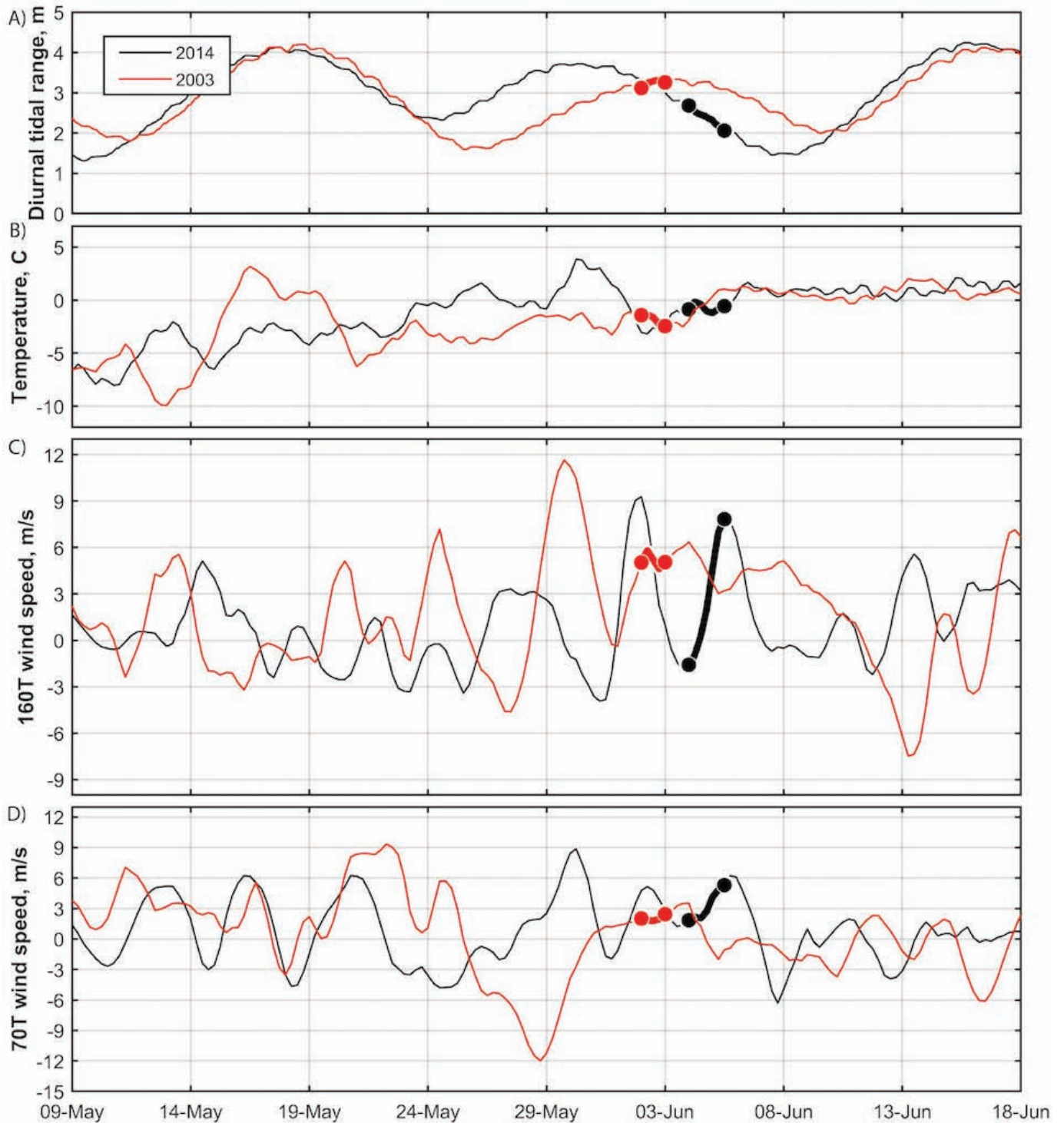


FIG. 15. Time series of the A) daily tidal range (m), B) air temperature ($^{\circ}\text{C}$), C) along-channel and D) across-channel winds (m/s) around the time of bridge breakup in Frozen Strait in 2003 and 2014. The thick lines highlight the timing of breakup and the dots show the start and end of the window.

CONCLUSIONS

The intermittent formation of an ice bridge across RWS is a unique feature of the Hudson Bay icescape that allows Inuit from Coral Harbour to cross the channel and hunt around Wager Bay and may provide a migration route for caribou onto Southampton Island. The first recorded

observation of the ice bridge that we were able to find is from a whaling vessel in August 1879, although Inuit have likely used the ice bridge for much longer considering that Paleo-Inuit inhabited the area around RWS as far back as 2500 BC. Presently, Inuit from Coral Harbour still use the ice bridge but know that the bridge only forms approximately every four years. Inuit know that the formation of the

bridge is tied to currents and air temperatures, however the mechanism by which the bridge forms has been unknown. Therefore, in this study we build off of local knowledge and provide the first scientific examination of the bridge, specifically examining how the bridge forms and breaks up; we subsequently speculate on why it forms so intermittently. Through a combination of satellite imagery and the archive of ice charts, we determined that from 1971 to 2020, a stable ice bridge formed across RWS 14 times. Three additional bridges temporarily formed between 2000 and 2020, though they collapsed within a few days of formation. Those bridges that were stable remained intact for over four months, breaking up between mid-June and early July after air temperatures had surpassed 0°C and the ice cover had begun to melt.

An analysis of the tidal and atmospheric forcing around the formation of the seven bridges that have formed since 2000 reveals typical conditions around the time of bridge formation:

1. *Cold air temperatures*: Bridges tend to form during prolonged periods of very cold air temperatures when temperatures are below -25°C and the 5-day FDD exceeds 140.
2. *Low tidal range*: Five of the seven recent bridges, including the four stable bridges, formed around neap tide when the daily tidal range was below 5 m.
3. *A rotation from northerly to west-northwesterly winds*: Prior to formation there is a reduction in along-channel winds and an increase in across-channel winds as the wind field rotates to a west-northwesterly direction.

In terms of the ice cover and formation of the bridge, these three factors combine to compress and immobilize the existing ice pack within RWS against Southampton Island. The ice cover then coalesces under cold air temperatures and is locked in place by rapid new ice formation on the west side of the channel, which is estimated to reach 24 cm in the eight days around formation. It is also required that along-channel wind speeds remain calm for several days after formation, allowing the bridge to stabilize. If winds increase too soon after formation, the bridge may collapse; if the bridge forms too far south (south of Ell Bay), it will not stabilize. Compression of the existing deformed ice pack and formation of a band of new ice through the western end of the bridge are evident from radar imagery of the bridges and confirmed through an across-channel gradient in ice freeboard (thickness). A shoal that is less than 20 m deep in the eastern part of the channel may also promote bridge formation if deep ridges become grounded and provide an anchor for the bridge, but it remains unclear if such thick ridges are formed within RWS. Once in place, the bridge strengthens thermodynamically and only breaks apart once air temperatures have risen to 0°C and the ice begins to warm and therefore weaken, as indicated by the formation of surface melt features across the bridge during June. Once

surface melt has begun, strong winds can cause the bridge to break up earlier; therefore, once surface melt begins, it is advisable that the ice bridge no longer be used to cross RWS. Throughout the observational record, the stable ice bridges broke up between mid-June and early July, although a historical account from 1879 indicates the bridge was in place into the first week of August. This difference in time of breakup may indicate a long-term change towards earlier breakup, a trend which has been observed in this area during the more recent satellite era (Andrews et al., 2018)

Given that it is impossible to predict exactly when the next ice bridge will form, it is important that any future in situ study of the bridge be a collaborative effort between scientists and Inuit from Coral Harbour who will be the first to observe the bridge when it forms. Since the longest observed period without a bridge is eight years, we expect a bridge to form before 2028. To understand the mechanisms related to the bridge itself, in situ observations of wind speeds and currents would provide insight into the forces acting on the bridge and therefore the strength of the bridge. Ice thickness surveys would support the notion of a cross-bridge gradient in ice thickness, while targeted ice thickness sampling coupled with water depth soundings around the shoals would reveal exactly how deep the shoals are and if grounded ridges contribute to the stabilization of the bridge. Additional observations of wildlife tracks, particularly caribou, would reveal how the bridge affects local wildlife. Further studies of the bridge would not only help to understand how the bridge forms and remains stable, but will also improve predictions for how climate change may affect this bridge and Inuit who rely upon it to travel to hunting grounds and ancestral locations around Wager Bay.

ACKNOWLEDGEMENTS

The authors thank the community of Coral Harbour, particularly the Elders and hunters who have shared their knowledge of the ice bridge (*Nunniq*) through interviews with different groups over the years. Thank you to the Aiviit Hunters and Trappers Organization in Coral Harbour, particularly N.H. Ottokie. Thank you to M. Yank from the Ukkusiksalik National Park office in Naujaat for sharing his knowledge and experience. Thank you to M. Mahy and A. Chagnon-LaFortune from Parks Canada for reviewing and providing constructive comments on the manuscript. Thank you to T. Loewen and S. Ferguson from the Department of Fisheries and Oceans Canada and J. Higdon from the University of Manitoba and Higdon Wildlife Consulting for sharing their knowledge of the area and providing feedback while the paper was being written. Thank you to A. Komarov from Environment and Climate Change Canada for assistance with RADARSAT imagery. Z. Kuzyk, J. Ehn, and M. Kamula wish to thank Parks Canada, Government of Nunavut, ArcticNet, and Polar Knowledge Canada, which have supported the research through which we built relationships with hunters near Naujaat and Coral Harbour. D. Babb, Z. Kuzyk, J. Ehn, and D. Barber would

like to thank the Natural Sciences and Engineering Research Council of Canada for financial support. D. Babb is additionally supported by the Canadian Meteorological and Oceanographic Society (CMOS). J. Liesch gratefully acknowledges the financial

support provided by the Northern Scientific Training Program and the W. Garfield Weston Foundation. Lastly, thank you to the editor, M. Plante, and an anonymous reviewer for providing valuable comments that helped improve this paper.

REFERENCES

- Agnew, T., Lambe, A., and Long, D. 2008. Estimating sea ice area flux across the Canadian Arctic Archipelago using enhanced AMSR-E. *Journal of Geophysical Research: Oceans* 113, C10011.
<https://doi.org/10.1029/2007JC004582>
- Amante, C., and Eakins, B.W. 2009. ETOPO1 1 arc-minute global relief model: Procedures, data sources and analysis. NOAA Technical Memorandum NESDIS NGDC-24. Boulder, Colorado: National Geophysical Data Center.
<https://doi.org/10.7289/V5C8276M>
- Andrews, J., Babb, D.G., and Barber, D.G. 2018. Climate change and sea ice: Shipping in Hudson Bay, Hudson Strait, and Foxe Basin (1980–2016). *Elementa: Science of the Anthropocene* 6(1): 19.
<https://doi.org/10.1525/elementa.281>
- Barbedo, L., Bélanger, S., and Tremblay, J.-É. 2020. Climate control of sea-ice edge phytoplankton blooms in the Hudson Bay system. *Elementa: Science of the Anthropocene* 8(1): 039.
<https://doi.org/10.1525/elementa.039>
- Barber, D.G., and Massom, R.A. 2007. The role of sea ice in Arctic and Antarctic polynyas. In: Smith, W.O., Jr., and Barber, D.G., eds. *Polynyas: Windows to the world's oceans*. Amsterdam: Elsevier. 1–54.
- Barber, D.G., Harasyn, M.L., Babb, D.G., Capelle, D., McCullough, G., Dalman, L.A., Mathes, L.C., et al. 2021. Sediment-laden sea ice in southern Hudson Bay: Entrainment, transport, and biogeochemical implications. *Elementa: Science of the Anthropocene* 9(1): 00108.
<https://doi.org/10.1525/elementa.2020.00108>
- BIO (Bedford Institute of Oceanography). 2020. WebTide tidal prediction model. Dartmouth, Nova Scotia: BIO.
www.bio.gc.ca/science/research-recherche/ocean/webtide/index-en.php
- Bruneau, J., Babb, D., Chan, W., Kirillov, S., Ehn, J., Hanesiak, J., and Barber, D.G. 2021. The ice factory of Hudson Bay: Spatiotemporal variability of the Kivalliq polynya. *Elementa: Science of the Anthropocene* 9(1): 00168.
<https://doi.org/10.1525/elementa.2020.00168>
- Campbell, M., Boulanger, J., and Lee, D.S. 2020. Long-term trends in abundance and distribution of the Southampton Island caribou herd: 1978–2019. Iqaluit: Department of Environment, Government of Nunavut.
- Campbell, N.J. 1964. The origin of cold high-salinity water in Foxe Basin. *Journal of the Fisheries Research Board of Canada* 21(1):45–55.
<https://doi.org/10.1139/f64-006>
- Canadian Ice Service. 2005. MANICE: Manual of standard procedures for observing and reporting ice conditions, 9th ed. Ottawa: Canadian Ice Service, Environment Canada.
https://publications.gc.ca/collections/collection_2013/ec/En56-175-2005-eng.pdf
- Candlish, L., Babb, D.G., Andrews, J., Myers, P.G., Ridenour, N., Landy, J.C., and Ehn, J.K. 2019. Characteristics of the seasonal sea ice cover. In: Kuzyk, Z.A., and Candlish, L.M., eds. *From science to policy in the greater Hudson Bay marine region: An integrated regional impact study (IRIS) of climate change and modernization*. Québec City: ArcticNet.
<https://arcticnet.ulaval.ca/publication-database/>
- Cooley, S.W., Ryan, J.C., Smith, L.C., Horvat, C., Pearson, B., Dale, B., and Lynch, A.H. 2020. Coldest Canadian Arctic communities face greatest reductions in shorefast sea ice. *Nature Climate Change* 10(6):533–538.
<https://doi.org/10.1038/s41558-020-0757-5>
- Copernicus Climate Change Service (C3S). 2017. ERA5: Fifth generation of ECMWF atmospheric reanalysis of the global climate. Reading, United Kingdom: European Centre for Medium-Range Weather Forecasts.
- Cosens, S.E., and Innes, S. 2000. Distribution and numbers of bowhead whales (*Balaena mysticetus*) in northwestern Hudson Bay in August 1995. *Arctic* 53(1):36–41.
<https://doi.org/10.14430/arctic832>
- COSEWIC (Committee on the Status of Endangered Wildlife in Canada). 2016. COSEWIC assessment and status report on the caribou (*Rangifer tarandus*), barren-ground population in Canada. Ottawa: COSEWIC.
- Defossez, M., Saucier, F.J., Myers, P.G., Caya, D., and Dumais, J.-F. 2008. Multi-year observations of deep water renewal in Foxe Basin, Canada. *Atmosphere–Ocean* 46(3):377–390.
<https://doi.org/10.3137/ao.460306>

- Desjardins, S.P.A. 2020. Neo-Inuit strategies for ensuring food security during the Little Ice Age climate change episode, Foxe Basin, Arctic Canada. *Quaternary International* 549:163–175.
<https://doi.org/10.1016/j.quaint.2017.12.026>
- DFO (Fisheries and Oceans Canada). 2011. Identification of ecologically and biologically significant areas (EBSA) in the Canadian Arctic. Science Advisory Report 2011/055. Ottawa: Canadian Science Advisory Secretariat, DFO.
<https://waves-vagues.dfo-mpo.gc.ca/Library/344747.pdf>
- . 2020. Proceedings of the regional science peer review on the biophysical and ecological overview of the Southampton Island ecologically and biologically significant area. Proceedings Series 2020/014. Winnipeg, Manitoba: Canadian Science Advisory Secretariat, DFO.
<https://waves-vagues.dfo-mpo.gc.ca/Library/40935954.pdf>
- Environment and Climate Change Canada. 2020. Ice thickness program collection, 1947–2002. Ottawa: Government of Canada.
<https://open.canada.ca/data/en/dataset/054cb024-e0bc-43ae-90c7-d9e23517ab8e>
- Ferguson, S.H., Higdon, J.W., and Chmelnitsky, E.G. 2010. The rise of killer whales as a major Arctic predator. In: Ferguson, S.H., Loseto, L.L., and Mallory, M.L., eds. *A little less Arctic: Top predators in the world's largest northern inland sea, Hudson Bay*. Dordrecht: Springer. 117–136.
https://doi.org/10.1007/978-90-481-9121-5_6
- Frasier, T.R., Petersen, S.D., Postma, L., Johnson, L., Heide-Jørgensen, M.P., and Ferguson, S.H. 2020. Abundance estimation from genetic mark-recapture data when not all sites are sampled: An example with the bowhead whale. *Global Ecology and Conservation* 22: e00903.
<https://doi.org/10.1016/j.gecco.2020.e00903>
- Gilder, W.H. 1881. *Schwatka's search: Sledging in the Arctic in quest of the Franklin records*. New York: Charles Scribner's Sons.
- Government of Nunavut. 2014. Nunavut coastal resource inventory: Coral Harbour. Iqaluit: Department of Environment.
https://www.gov.nu.ca/sites/default/files/ncri_coral_harbour_en.pdf
- Hannah, C.G., Dupont, F., and Dunphy, M. 2009. Polynyas and tidal currents in the Canadian Arctic Archipelago. *Arctic* 62(1):83–95.
<https://doi.org/10.14430/arctic115>
- Heide-Jørgensen, M.P., Burt, L.M., Hansen, R.G., Nielsen, N.H., Rasmussen, M., Fossette, S., and Stern, H. 2013. The significance of the North Water polynya to Arctic top predators. *Ambio* 42(5):596–610.
<https://doi.org/10.1007/s13280-012-0357-3>
- Hibler, W.D., III, Hutchings, J.K., and Ip, C.F. 2006. Sea-ice arching and multiple flow states of Arctic pack ice. *Annals of Glaciology* 44:339–344.
<https://doi.org/10.3189/172756406781811448>
- Higdon, J.W., and Ferguson, S.H. 2010. Past, present, and future for bowhead whales (*Balaena mysticetus*) in northwest Hudson Bay. In: Ferguson, S.H., Loseto, L.L., and Mallory, M.L., eds. *A little less Arctic: Top predators in the world's largest northern inland sea, Hudson Bay*. Dordrecht: Springer. 159–177.
https://doi.org/10.1007/978-90-481-9121-5_8
- Howell, S.E.L., Derksen, C., Pizzolato, L., and Brady, M. 2015. Multiyear ice replenishment in the Canadian Arctic Archipelago: 1997–2013. *Journal of Geophysical Research: Oceans* 120(3):1623–1637.
<https://doi.org/10.1002/2015JC010696>
- Inuit Heritage Trust. 2016. Place names program. Iqaluit: IHT.
<http://iht.ca/eng/place-names/pn-goog.html>
- Kirillov, S., Babb, D.G., Komarov, A.S., Dmitrenko, I., Ehn, J.K., Worden, E., Candlish, L., Rysgaard, S., and Barber, D.G. 2021. On the physical settings of ice bridge formation in Nares Strait. *Journal of Geophysical Research: Oceans* 126(8): e2021JC017331.
<https://doi.org/10.1029/2021JC017331>
- Kubat, I., Sayed, M., Savage, S.B., and Carrieres, T. 2006. Flow of ice through converging channels. *International Journal of Offshore and Polar Engineering* 16(4):268–273.
- Kwok, R. 2005. Variability of Nares Strait ice flux. *Geophysical Research Letters* 32(24): L24502.
<https://doi.org/10.1029/2005GL024768>
- . 2007. Baffin Bay ice drift and export: 2002–2007. *Geophysical Research Letters* 34(19): L19501.
<https://doi.org/10.1029/2007GL031204>
- Kwok, R., Pedersen, L.T., Gudmandsen, P., and Pang, S.S. 2010. Large sea ice outflow into the Nares Strait in 2007. *Geophysical Research Letters* 37(3): L03502.
<https://doi.org/10.1029/2009GL041872>
- Kwok, R., Markus, T., Kurtz, N.T., Petty, A.A., Neumann, T.A., Farrell, S.L., Cunningham, G.F., Hancock, D.W., Ivanoff, A., and Wimert, J.T. 2019. Surface height and sea ice freeboard of the Arctic Ocean from ICESat-2: Characteristics and early results. *Journal of Geophysical Research: Oceans* 124(10):6942–6959.
<https://doi.org/10.1029/2019jc015486>

- Kwok, R., Cunningham, G.F., Markus, T., Hancock, D.W., Morison, J.H., Palm, S., Farrell, S.L., Ivanoff, A., Wimert, J., and the ICESat-2 Science Team. 2020. ATLAS/ICESat-2 L3A sea ice height, Version 3. Boulder, Colorado: National Snow & Ice Data Center.
<https://doi.org/10.5067/ATLAS/ATL07.003>
- Laidler, G.J., Dialla, A., and Joamie, E. 2008. Human geographies of sea ice: Freeze/thaw processes around Pangnirtung, Nunavut, Canada. *Polar Record* 44(4):335–361.
<https://doi.org/10.1017/S003224740800750X>
- Landy, J.C., Ehn, J.K., Babb, D.G., Thériault, N., and Barber, D.G. 2017. Sea ice thickness in the eastern Canadian Arctic: Hudson Bay complex & Baffin Bay. *Remote Sensing of Environment* 200:281–294.
<https://doi.org/10.1016/j.rse.2017.08.019>
- Larouche, P., and Galbraith, P.S. 1989. Factors affecting fast-ice consolidation in southeastern Hudson Bay, Canada. *Atmosphere–Ocean* 27(2):367–375.
<https://doi.org/10.1080/07055900.1989.9649341>
- Lebedev, V.V. 1938. Rost l'da v arkticheskikh rekakh i moriakh v zavisimosti ot otritsatel'nykh temperatur vozdukh [Growth of ice in Arctic rivers and seas in relation to negative air temperature]. *Problemy arktiki [Arctic Proceedings]* 5(6):9–25.
- Markham, W.E. 1986. The ice cover. In: Martini, I.P., ed. *Canadian inland seas*. Amsterdam: Elsevier Oceanography Series, Vol. 44. 101–116.
- Matthes, L.C., Ehn, J.K., Dalman, L.A., Babb, D.G., Peeken, I., Harasyn, M., Kirillov, S., et al. 2021. Environmental drivers of spring primary production in Hudson Bay. *Elementa: Science of the Anthropocene* 9(1): 00160.
<https://doi.org/10.1525/elementa.2020.00160>
- Nunavut Wildlife Management Board. 2020. Status of the Southampton Island barren-ground caribou population (July 2020).
<https://www.nwmb.com/iku/2013-11-09-01-41-51/2013-11-09-01-47-14/regular-meetings/2020-1/rm-004-2020-december-2-2020/english-13/8375-tab3a-gn-bn-southampton-island-caribou-eng>
- Parker, G.R. 1975. An investigation of caribou range on Southampton Island, NWT. Canadian Wildlife Service Report Series 33. Ottawa: Environment Canada, Wildlife Service.
<http://parkscanadahistory.com/wildlife/report-33.pdf>
- Parks Canada. 2018. Ukkusiksalik National Park of Canada: Management plan. Ottawa: Parks Canada.
<https://www.pc.gc.ca/en/pn-np/nu/ukkusiksalik/info/index/gestion-management-2018>
- Pierrejean, M., Babb, D.G., Maps, F., Nozais, C., and Archambault, P. 2020. Spatial distribution of epifaunal communities in the Hudson Bay system: Patterns and drivers. *Elementa: Science of the Anthropocene* 8(1): 00044.
<https://doi.org/10.1525/elementa.00044>
- Prach, R.W., Boyd, H., and Cooch, F.G. 1981. Polynyas and sea ducks. In: Stirling, I., and Cleator, H., eds. *Polynyas in the Canadian Arctic*. Occasional Paper No. 45. Ottawa: Canadian Wildlife Service. 67–70.
https://publications.gc.ca/collections/collection_2018/eccc/CW69-1-45-eng.pdf
- Price, R. 1970. *The howling Arctic: The remarkable people who made Canada sovereign in the farthest North*. Toronto: Peter Martin & Associates.
- Prinsenber, S. 1986. The circulation pattern and current structure of Hudson Bay. In: Martini, I.P., ed. *Canadian inland seas*. Amsterdam: Elsevier Oceanography Series, Vol. 44. 187–204.
- Rallabandi, B., Zheng, Z., Winton, M., and Stone, H.A. 2017. Formation of sea ice bridges in narrow straits in response to wind and water stresses. *Journal of Geophysical Research: Oceans* 122(7):5588–5610.
- Richard, P.R., Orr, J.R., and Barber, D.G. 1990. The distribution and abundance of belugas, *Delphinapterus leucas*, in eastern Canadian Subarctic waters: A review and update. In: Smith, T.G., St. Aubin, D.J., and Geraci, J.R., eds. *Advances in research on the beluga whale, Delphinapterus leucas*. Canadian Bulletin of Fisheries and Aquatic Sciences 224. 23–38.
<https://waves-vagues.dfo-mpo.gc.ca/Library/119072.pdf>
- Ross, W.G. 1974. Distribution, migration, and depletion of bowhead whales in Hudson Bay, 1860 to 1915. *Arctic and Alpine Research* 6(1):85–98.
<https://doi.org/10.2307/1550373>
- Saucier, F.J., Senneville, S., Prinsenber, S., Roy, F., Smith, G., Gachon, P., Caya, D., and Laprise, R. 2004. Modelling the sea ice-ocean seasonal cycle in Hudson Bay, Foxe Basin and Hudson Strait, Canada. *Climate Dynamics* 23(3-4):303–326.
<https://doi.org/10.1007/s00382-004-0445-6>
- Savelle, J.M., and Dyke, A.S. 2014. Paleoeskimo occupation history of Foxe Basin, Arctic Canada: Implications for the Core Area Model and Dorset origins. *American Antiquity* 70(2):249–276.
<https://doi.org/10.7183/0002-7316.79.2.249>
- Sodhi, D.S. 1977. *Ice arching and the drift of pack ice through restricted channels*. Hanover, New Hampshire: Cold Regions Research and Engineering Lab.
- Stirling, I., and Cleator, H. 1981. *Polynyas in the Canadian Arctic*. Occasional Paper No. 45. Ottawa: Canadian Wildlife Service.

- Taha, W., Bonneau-Lefebvre, M., Cueto Bergner, A., and Tremblay, A. 2019. Evolution from past to future conditions of fast ice coverage in James Bay. *Frontiers in Earth Science* 7: 254.
<https://doi.org/10.3389/feart.2019.00254>
- Tivy, A., Howell, S.E.L., Alt, B., McCourt, S., Chagnon, R., Crocker, G., Carrieres, T., and Yackel, J.J. 2011. Trends and variability in summer sea ice cover in the Canadian Arctic based on the Canadian Ice Service Digital Archive, 1960–2008 and 1968–2008. *Journal of Geophysical Research: Oceans* 116: C03007.
<https://doi.org/10.1029/2009JC005855>
- Ukkusiksalik Inuit Working Group, Mouland, G., and Manseau, M. 2013. Inuit knowledge of Ukkusiksalik National Park. Ottawa: Parks Canada.
- Vincent, R.F. 2019. A study of the North Water Polynya ice arch using four decades of satellite data. *Scientific Reports* 9(1): 20278.
<https://doi.org/10.1038/s41598-019-56780-6>